

# Novel trends in resilience assessment of a distribution system using synchrophasor application: A literature review

Sonal  | Debomita Ghosh 

Department of EEE, Birla Institute of Technology Mesra, Ranchi, India

## Correspondence

Sonal, Department of EEE, Birla Institute of Technology Mesra, Ranchi, India.  
Email: phdee10001.19@bitmesra.ac.in

**Handling AE:** Li, Ran

## Summary

The gradual sprawl of power system toward smart grid and enhanced integration of distributed energy resources at the distribution end is transforming the conventional distribution system and is eventually making it self-sustained. The distribution system is thus continuously evolving to prepare itself for any unforeseen natural, man-made, and complex events. These events may impact the distribution system as high-impact low-frequency (HILF) scenarios. The high intensity and widespread damage of the power system due to HILF scenarios necessitate resilience. Resilience analysis aims to identify these region-specific vulnerabilities of the electricity network and implement appropriate methods to quickly restore the system to its predisturbance state. Further to enhance the network visibility and situational awareness, integration of synchrophasor to resilience is significant. Therefore, synchrophasor technology integrated with resilience provides online wide area visibility of the distribution system. Using synchrophasor for resilience assessment propels an agile network for coordinating accurate and timely analysis of the system parameters. Therefore, understanding the concept of resilience, its evolution, detailed overview, synchrophasor-based resilience (SBR) methods as well as its applications are necessary. This article outlines the key points of the synchrophasor technology based resilience technique, its significance, and lays a foundation for continuing research in this area. It offers detailed insight into the comprehensive review of this evolving concept. The article majorly focuses on all the aspects of SBR, its necessity in performance evaluation, synchrophasor

**Abbreviations:** HILF, High impact low frequency; WAMS, Wide-area monitoring system; SA, Situational awareness; ROCOF, Rate of change of frequency; PDC, Phasor data concentrator; SBR, Synchrophasor-based resilience; Res, Resilience; NIAC, National infrastructure advisory council; PCA, Principal component analysis; SS, Similarity search; RPCA, Recursive principal component analysis; WLAV, Weighted least absolute value; ALM, Augmented Lagrangian multiplier; BC, Bayesian classifier; PMU, Phasor measurement unit; D-PMU, Distribution phasor measurement unit; DG, Distributed generation; SDNAE, Stacked de-noising auto encoder; CPR, Cyber-physical resilience; WMSR, Weighted mean subsequence reduced; SC, Secondary control; DUDM, Data unavailability detector module; FR, Frame rate; ALDC, Adaptive lossless data compression; RCAM, Rot cause analyzer module; DMM, DoS mitigation module; LOF, Local outlier factor; DNN, Deep neural network; FDI, False data injection; SSL, Semi-supervised learning; DER, Distributed energy resource; GPS, Global positioning system; TVE, Total vector error; CI, Choquet integral; SILP, Small integer linear programming; DoS, Denial of service; EC, Event-centered; RC, Response-centred; ML, Machine learning; KNN, K-nearest neighbors; PS, Power system; CB, Circuit breaker; SE, State estimation; FDIA, False data injection attack.

measurement based resilience enhancement methods, and application of different SBR techniques in the distribution system. A detailed comparative analysis of SBR features, sample efficiency, result accuracy, merits, and demerits based on available literature is provided. Finally, future perspectives are discussed for implementing resilience assessment using synchrophasor technology in the distribution system.

#### KEYWORDS

distributed energy resources, high-impact low-frequency, resilience, situational awareness, synchrophasor, wide-area monitoring system

## 1 | INTRODUCTION

The power system being outdoor is vulnerable to high-impact low-frequency (HILF) events such as earthquakes, storms, regional floods, physical attacks, and so on. These different vulnerabilities make both the transmission and distribution systems susceptible to damage due to HILF events. Resilience is the ability of a system to adapt and timely react to such HILF events. It is an evolving framework to address extreme events.<sup>1</sup> With the increase in awareness of these events, resilience has become important worldwide.<sup>2</sup> The intensity, severity, and exposure of the network to extreme conditions determine the resilience measures to be adopted. These resilience measures are broadly classified into short-term and long-term strategies.<sup>3</sup> The most appropriate resilience strategy depends on the source of HILF interruptions, their severity, and the extent of damage assessment to the network.<sup>4,5</sup> The analysis of these experiences is vital in determining the resilience measures. Table 1 highlights the power interruptions and severity details due to HILF events worldwide.

Table 1 Power system severity details due to HILF events worldwide (2010-2020).<sup>4,27</sup> The sprawl of conventional distribution system with huge integration of DERs has increased its self sustenancy and also made it more complex. Thus, for the distribution system, the topographic attributes and presence of different DERs aggravate the chances of impact due to HILF events. Keeping in view both the aspects, resilience in distribution system is essential so that self sustenancy of the network can be maintained. With the increase in HILF events, resilience is becoming increasingly important for the gradually maturing distribution system. Risk based resilience metrics can lead to life-cycle enhancement of the aging distribution system.<sup>6</sup> As many as 90% interruptions experienced by the customer are due to weather phenomena. In<sup>7</sup> distribution system resilience under different weather scenarios using time-to-event models is assessed. Matrix based approach and probabilistic metrics quantify the operational resilience due to HILF events. It identifies the potential risks and finds possible routes of recovery after the impact.<sup>8,9</sup> Linear programming optimization is suggested for resilience driven energy storage system planning.<sup>10</sup> For wind powered system, an ordered curtailment strategy ensures grid resilience during cyclone Typhoon.<sup>11</sup> Many a time, lack of information such as uncertain HILF characteristics make it difficult to evaluate distribution system resilience.<sup>12</sup> This necessitates effective SA and improved observability at all times. The growing significance of DERs has led to a new level of uncertainty. The challenges of power system resilience due to high DER penetration are discussed in.<sup>13</sup> In<sup>14</sup> a comprehensive study of all types of resilience metrics is presented. This conceptual framework considers physical, cyber, cyber-physical components, as well as personnel involved in extreme conditions. Most of the previous works have focused more on resilience quantification. A comprehensive analysis of effective mitigation perspectives of distribution system using synchrophasor application is not presented. Also, the lack of SA in the distribution side delays the timely response and poses a challenge to the distribution system resilience. Deploying synchrophasor technology provides insight into the distribution system conditions at all times. Distribution side operators can use this information for better visibility of grid events and its performance during HILF events. It increases the accuracy and usefulness of resilience analysis.

This article presents a detailed overview of distribution system resilience based on synchrophasor measurement. It includes the evolution of synchrophasor-based resilience (SBR) in the distribution system, its overview, related framework, and recent developments. The prime focus is on SBR implementation methods, and synchrophasor based application in distribution system resilience assessment. Finally, a comparative assessment of the existing SBR analysis techniques applied in the distribution system is provided and new research perspectives for synchrophasor based grid resilience monitoring and control is proposed.

**TABLE 1** Power system severity details of HILF events worldwide (2010-2020)<sup>4,27</sup>

Origin	Category	Type	Region	Year	Mean customers affected (thousand)	Mean outage duration	
Natural	Metrological	Windstorm	U.S.A	2010-17	750 000	2.5 days	
			Europe	2010-17	1 900 000	409 min	
			Australia	2010-15	1700	4 days	
			Philippines	2014	64 900	2-5 days	
			India	2014	277	36-48 h	
			Puerto Rico	2017	1750	1 month	
			England	2017	1800	5-6 days	
			Ice storm	U.S.A	2010	200	0.5- days
				Ireland	2010	30	Several days
		Poland		2013	100	3-4 days	
		Lightning	U.S.A	2017	70	Few hours	
			Heat wave	South Korea	2011	9000	2 h
			Geological	Earthquake	New Zealand	2010-17	160
		India			2017	93 000	1-2 days
		Japan			2018	2950	2-3 days
Unintentional/Technical/ External	Accidental	Fire/ explosion			Cyprus	2011	30
			Australia	2019	76	2 days	
			Crimea	2015	1200	Few hours	
			Venezuela	2018	17	18 h	
Human Intentional	Malicious acts	Intentional attack	USA	2014	24	Few hours	
			Ukraine	2016	230	1-6 h	

The remaining manuscript is organized as follows: Section 2 deals with the evolution of SBR in the distribution system, Section 3 enlists the HILF exposure and causes, and Section 4 discusses the significance of SBR and its implementation. Methodologies for SBR implementations are detailed in Section 5, and Section 6 analyzes the synchrophasor based application in distribution system resilience assessment. Section 7 compares the different SBR analysis techniques, followed by future research perspectives in Section 8. Section 9 concludes the survey.

## 2 | EVOLUTION OF RESILIENCE IN DISTRIBUTION SYSTEM BASED ON SYNCHROPHASOR TECHNOLOGY

The term “resilience” was first coined in 1973 by a notable researcher C.S Holling.<sup>2</sup> He was the prime person behind the foundational interpretation of resilience. Researchers made several attempts to generalize this concept in diverse fields.

The United Nations proposed a general multidisciplinary definition of resilience. It defines resilience as the capability to suitably resist and subsume flexibly.<sup>15</sup> This means increasing the system’s capacity to manage the impact of HILF events and recovering rapidly from the implications caused by it. The framework for timely recovery against adverse scenario outlines these basic functionalities and related operating criteria of network.

The concept of resilience goes beyond quality, flexibility, and robustness. These fundamental terms just express the technical and physical aspects of infrastructure. Stability is an important aspect of the power system related to resilience. Stability refers to the ability of a system to perform its intended function. It points out how long the system can hold its performance intact before getting disrupted. The more perturbations it can handle, it is said to be more stable. Being stable prevents the system to proceed into any state of disturbance, while resilience is the capability of the system

RESILIENCE FEATURES	DEFINITION
Flexibility	The ability of a network to easily modified according to the external changes in the system behaviour
Adaptability	The property of a system to adjust or fit the new systemic changes in the advent of HILF events
Robustness	The quality of a system to withstand or overcome adverse conditions with a satisfactory measure of performance
Redundancy	A feature of a system to have options for inclusion in the advent of stressful scenarios faced by it
Capacity	The behaviour of a system by which it can absorb maximum unexpected disturbances
Interoperability	The quality of a system to exchange and make use of data sharing to access and use information in a coordinated manner within the system
Longevity	It is a concept related to long retaining functionality or service by the system and satisfactorily provides load demands of customers
Rapid Recovery	The property of a system to quickly recover back to its pre-disturbance state with timely and easy reorganization itself

FIGURE 1 Generic features of resilience and its definition

to quickly recover to its predisturbance state due to the impact of HILF events. Resilience highlights the preparedness to handle disruptions, sudden network interruptions, and abnormal scenarios that might push the system to an unstable state affecting its normal operation. It reflects the potential to deal with the changes in the system till it becomes irrevocable.<sup>15</sup> It shows how well the system can cope up with the consequences of catastrophic failure. More the coping ability, the system is said to be more resilient. The HILF events have uncertainties associated with them due to changing climate, technology, and aging of systems. Therefore, withstanding the effect of all such changing conditions is an aspect of resilience.<sup>16</sup> Many researchers have outlined resilience against HILF conditions as the potential to alleviate the desired outcome. The National Infrastructure Advisory Council (NIAC) has incorporated some main features of the resilience framework, as shown in Figure 1. These key features form the essential underlying criteria of the resilience concept.<sup>5,17-22</sup>

The power system resilience concept has taken shape in and around the last decade.<sup>23</sup> For the security and adequacy aspect, reliability analysis is considered. But in the face of catastrophe, it was inadequate in capturing the system performance. This void in power system performance measurement required a different approach.<sup>24</sup> Also, the aging of the network made it difficult to handle the impact of extreme events. Enhancing resilience is a better option instead of replacing the whole network.<sup>25,26</sup> Thus, the integration of resilience with SBR is the key to better network restoration and monitoring. The gradual sprawl of conventional power system towards smart grid has led to the deployment of phasor measurement units (PMUs). PMUs can measure the change in power, voltage, phase angle, frequency and, rate of change of frequency (ROCOF) all in real-time. It monitors significant deviations in real-time synchrophasor measurement and records it with high accuracy. This high-speed monitoring avoids data reporting lag and enables overall better visibility to record grid events.<sup>7</sup> Application of synchrophasor in enhancing power system resilience enables easy and fast transfer of vital data that falls into three major categories (1) real-time monitoring, (2) disruption mitigation, and (3) non-network centric framework.<sup>27,28</sup> Resilience framework combined with synchrophasor detects mismatch of network parameters. It enhances SA and protects the system from any unpredictable condition.

Figure 2 represents the generic block scheme of SBR for distribution system. When HILF event hits the distribution system, the PMUs collect data pertaining to system states. These relatively smaller but significant deviations of real-time synchrophasor measurements are recorded with high accuracy. Further, the local phasor data concentrator (PDC) collects these distribution level information. PMUs and PDCs are connected via communication lines as illustrated in Figure 2. These synchrophasor data from several local PDCs are collected and shared with the regional PDCs to the control center. Historical data associated with similar events are compared with the synchrophasor data acquired to form a resilience goal. The grid parameters are thus effectively quantified. These are processed and analyzed to prepare the network for restoration activities.

Thus, SBR enhances SA and protects the system from any unpredictable condition. This type of real-time analysis helps in resilience based planning and implementation of network in a specific region.

## Synchrophasor based Resilience Implementation

## Synchrophasor based Resilience Planning

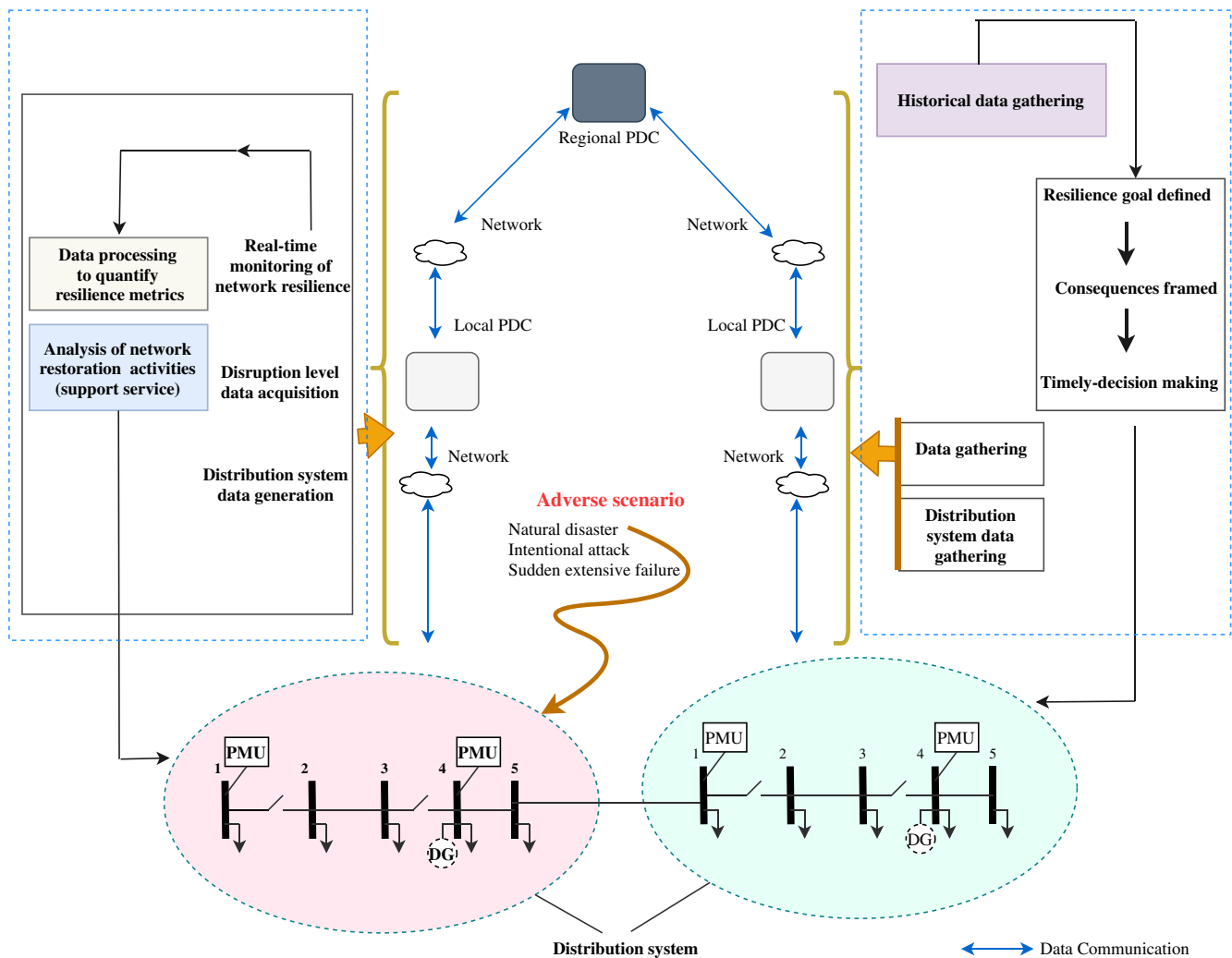


FIGURE 2 Scheme of generic synchrophasor based resilience for distribution system

### 3 | HILF EVENT AND CAUSES

Resilience based on synchrophasor technology aims at achieving a desired level of performance. It majorly focuses on real-time system information, event-detection, and recovery task. This type of framework is necessary for decision making and understanding the dynamics behind resilience implementation. There exists a wide gap in the practical implementation status of SBR applications in the existing power sectors around the world. Table 2 lists the most common HILF events and related resilience level requirements for better performance.

It shows the most affected nations and their estimated exposed capacity due to windstorms, earthquakes, floods, and cyber-attacks. The consequences on both the transmission and distribution sides are mentioned. These disruptions may have a medium impact on the exposed capacity for nations like Sudan, India, Fiji, Indonesia, and so on. whereas Bangladesh, El Salvador, and Mozambique have almost 90% exposed capacity. Most of the exposed capacity value falls within cent percent. A value more than 100% means that it is subjected to multi-hazards at the same time. As in Table 2, it is found that owing to the geographic location of Honduras, it is under the threat of both floods and hurricanes. The simultaneous exposure to one or more hazard, forces the system to exceed the critical threshold of installed capacity. The exposed capacity may face losses due to generator inundation, substation flooding, and heavy damage to equipment. Since 80% population resides in hilly terrains, these conditions get aggravated.

TABLE 2 Effect of HILF events and related resilience level requirements<sup>16,23,29,30</sup>

HILF event	HILF Exposure		Effect of HILF Event on	
	Most dominant region	Exposed capacity (approx.)	Transmission side	Distribution side
Wind-storm	Bangladesh	90%	Toppling of transmission lines	Damage to poles and lines
	Japan	40%		
	Taiwan	70%		
	India	61.8%		
Earth-quake	Japan	70%	Inadequate anchorage likely to destroy lines	Ground shaking damages UG/OH lines, poles
	Mozambique	85%		
	El Salvador	90%		
	India	90%		
Flood	Honduras	150%	Damage to sub-station and transformers due to inundation	Underground lines impairment due to seepage
	Fiji	60%		
	Sudan	40%		
	India	47%		
Cyber-attack	USA	20%	Overloading of transmission lines due to excess false data	Disrupting security and reliability by gaining access to substation
	Russia	46%		
	Indonesia	38%		
	China	30%		

### Distribution System Interruption Causes

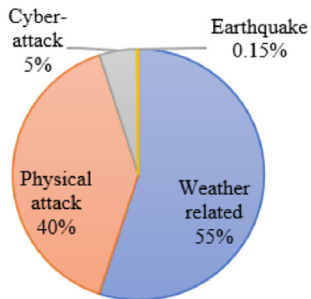
FIGURE 3 Distribution system interruption causes<sup>15,31</sup>

Figure 3 shows that almost every possible adverse condition is likely to impact the distribution system. It substantiates that resilience is vital for the distribution side. The last 10 years data show that the weather related and physical attacks account for the maximum number of interruptions. Weather related interruptions are 54.85%, physical attacks account for 40%, and cyber-attacks 5%. Earthquakes occur in few seismic zones, so these account for 0.15%.

The percentage of disruptions due to these extreme events makes the system vulnerable to failures. SBR aids in adaptation, and protection against further system degradation. Based on the effect and causes of disruption due to HILF events, SBR is classified. Figure 4 represents the classification of SBR based on these parameters. The classification considers damage expense, recovery time, and network flexibility. Any HILF event that is not properly handled usually leads to the partial or large expense of network damage. The goal of SBR is to address such events efficiently. While it is difficult to completely eradicate the possibility of damage, remedial actions help to minimize its effects. For this purpose, a response plan is prepared beforehand to handle the risks of future HILF incidents. These are collectively known as response-centred (RC) resilience actions. Under RC actions, threat

characterization and vulnerability assessment outlines the resilience level recommended for network components. To manage the aftermath of a HILF incident, quick decision along with timely restoration is needed, which falls in the category of event-centered (EC) resilience actions. These comprise operational actions, load prioritization, and DER control actions.

Table 3 represents the comparative assessment of RC and EC resilience. It contrasts the features of RC with EC based on corrective actions, resilience goals, adaptability, grid operators capabilities, and related measures to be followed. The preventive actions for RC include infrastructural assessment, weather information, connectivity analysis, and robustness enhancement. RC is preparedness to face unexpected abnormal scenarios in the future. EC measures are based on distribution system recovery ability during the HILF event. It includes support service, back-up facility, load management, and active warning system. Load management action comprises activities to reduce electricity consumption at critical times. It is not directly a storage technique but it can serve some storage functions, so at times it comes under response based mitigation of HILF event. But, more appropriately, it can be applied for event-centered actions because it can lead to improvement in critical demand characteristics during HILF incidents.

Based on the type of the distribution system resilience, identification, and mitigation measures for SBR are presented in Figure 5. These identification and mitigation requirements for RC and EC resilience types aim at system survivability and to efficiently adapt to the HILF disturbances.<sup>32</sup>

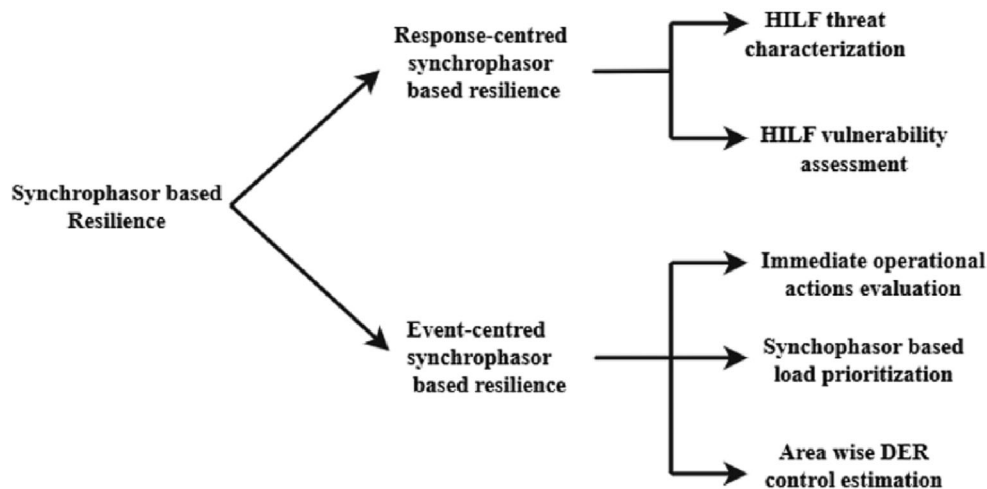


FIGURE 4 SBR classification

TABLE 3 Distribution system resilience type based on HILF events<sup>32</sup>

Response-centered resilience	Event-centered resilience
Corrective actions taken in advance to handle the impact of HILF events	Corrective actions taken aftermath of HILF to quickly minimize loss, mitigate the network from damage, and restore it
It consists of a set of best practices or response plan to reduce the risks before it causes damage	It consists of mitigative actions for quick decision to provide a timely system restoration
Proper planning and region-specific impact analysis framework results in fewer extensive damage to the system	It is associated with real-time quantification of network performance by applying lessons from similar past extreme conditions
Usually deals with grid planners and system analytics	Experienced personnel/ crew members handle such situations in a better way
Example: infrastructural assessment, weather intensity prior assessment, network connectivity analysis, robustness enhancement techniques etc.	Example: enhanced service support and back-up resource allocation, load-management activities, activation of warning system, etc.

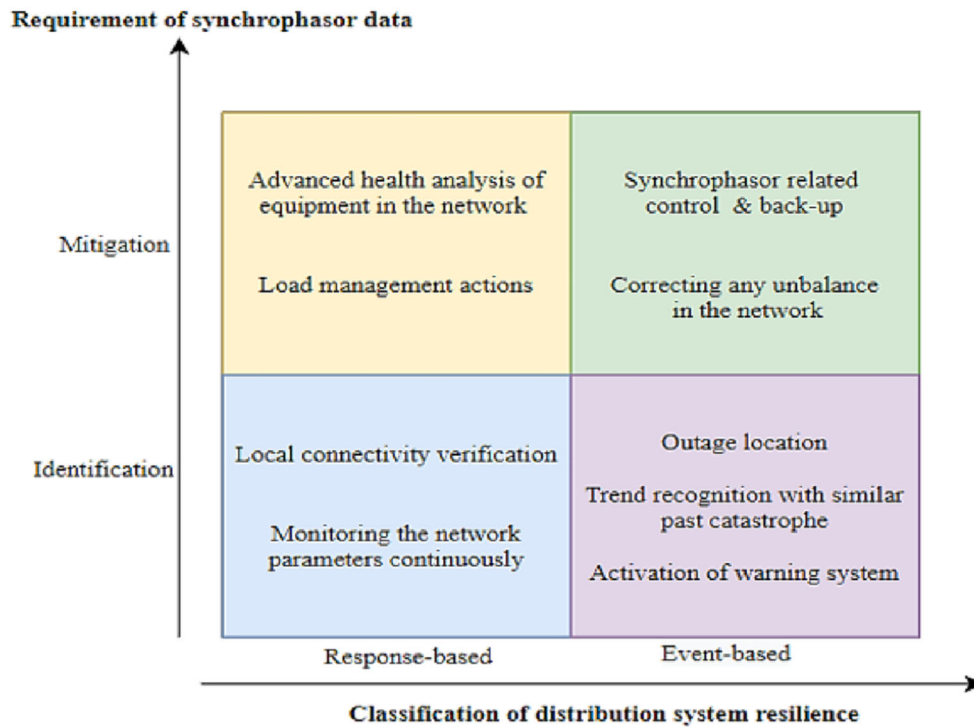


FIGURE 5 Identification and mitigation measures for response-centred (RC) and event-centered (EC) resilience

Resilience Benefits	Related Synchrophasor Parameters	Ref.
Fewer HILF outages	Improved situational awareness	20
Less HILF emergencies	Early detection and continuous monitoring	21,22
Lesser outage duration	Fast PMU preevent outage analysis	10,33,37
Fewer customers affected	Fast identification of disturbances	34
Faster restoration	Reduced equipment outage minutes and severity	35
Faster HILF event analysis	Real-time, accurate data reference from past lessons	3,36

TABLE 4 Synchrophasor based resilient distribution system benefits for HILF events

#### 4 | SIGNIFICANCE OF SBR AND ITS IMPLEMENTATION

Synchrophasor technology based resilience emerged when the US Department of Energy presented reports on blackouts and sudden consequences of power system interruption. It involves precise intrusion detection, accurate external threat monitoring, and perceiving the dangers of prolonged recovery activities.<sup>33,34</sup> The short and long-term power system resilience is addressed in ref. [35] In ref. [3,36] the benefits of incorporating the SBR approach to sustain the predisturbance state of distribution system are discussed.

Table 4 presents an organized walkthrough of advantages provided by SBR incorporated in the distribution system. SBR provides benefits like fewer outages, less emergency, less number of customers affected, faster restoration, and fast event analysis. Enhanced SA due to SBR enables greater observability to identify potential issues leading to fewer disruptions. Early detection and continuous monitoring helps to implement quick remedial measures. It leads to lesser emergency scenarios.<sup>38,39</sup> For fast preevent outage analysis, a sub-space of different HILF events established offline is compared with real-time PMU measurements. Combining PMU measurements with numerical sub-space of past HILF events identifies similar events encountered by the system. This data-driven outage identification reduces the computational time of the event analysis. It reduces the likelihood of longer outage duration during abnormal conditions.<sup>40</sup>

TABLE 5 SBR implemented in practical scenarios

Synchrophasor Application	Resilience Features	Data Reporting Rate (Hz)	Data Latency	Practical Network	Ref.
Situational awareness	System behavior under HILF	> 1	5 seconds	Netherlands Distribution Grid	38
State estimation	Real-time network degraded state estimation	< 1	1–5 seconds	EPFL, Switzerland	39
Synchro-check	Estimation of network elements unavailability in HILF scenarios	> 4	100 m seconds (ms)	Distribution feeder in Tehran	40
Oscillation detection	Preevent reconfiguration based on data anomaly	> 10	200 ms-1 second	Idaho falls, U.S.A	41
Voltage instability	Withstanding sudden voltage dip/swell in extreme weather	> 1	1–30 seconds	Portuguese Distribution System	42

The significance of SBR justifies its popularity and implementation in the distribution network. PMU allows resilient grid operation by efficient SA, state estimation, oscillation detection, instability analysis, and synchrophasor measurements condition-based validation.<sup>41</sup> Table 5 maps some practically implemented synchrophasor based resilient distribution network features.

The feature of small data latency leads to faster monitoring of system disruption. As a result, detecting and managing the impact of HILF events becomes easy. Also, a fast data reporting rate removes any lag between event analysis and related control actions. These SBR features improve the ability to visualize system dynamics, identify potential issues, and assess timely remedial measures.

## 5 | METHODS USED IN SBR EVALUATION

This section describes the SBR methodologies used for the distribution system. These methods are the SBR model approach, SBR data-driven approach, SBR machine learning approach, SBR quantification approach, and SBR miscellaneous approach. Table 6 portrays a detailed classification of these methods.

### 5.1 | SBR model approach

The detection of damage due to HILF event is based on well-suited algorithms to ensure a resilient and hassle-free operation of the distribution system. When the system encounters any abnormal event, the quality and quantity of power delivered to the customers get affected due to the operational degradation of the components. Addressing these system degradation using synchrophasor measurements on a suitable platform forms the basis of SBR model approach.

#### 5.1.1 | Robust principal component analysis (PCA) framework

A malicious data corruption resilience framework based on PCA of synchrophasor data, is proposed in ref. [45] The PCA algorithm preprocesses the synchrophasor measurements based on detected malicious data in cyber-attacks. The first step is  $l_2$  norm-fitting of the synchrophasor data  $x(t)$  from the set of measurements at time instant  $t$ , as in Equation (9). The steepest descent method followed by the convex optimization technique for preprocessing is performed by comparing the  $l_p$ -norm at  $p = 0.5$  and  $l_1$ -norm approach, as in Equations (1)–(3).

$$\min_{x(t)} = \|x(t)\|_2 \quad (1)$$

TABLE 6 Methods used in the implementation of SBR

Type	User Method	Ref.
SBR model approach	Denial-of-service resilient WAMS framework	43
	Distribution system state estimation framework	44
	Robust principal component analysis (PCA) framework	45
		46
	Similarity search-principal component analysis (SS-PCA) framework	47
	Augmented Lagrangian multiplier-based (ALM) algorithm	48
SBR data-driven approach	Network compensation theorem based method	49
	Hybrid state estimation based method	50
		51
	Improved robust-PCA based method	52
	Behavioral systems theory-based method	53
SBR machine learning approach	Bayesian classifier (BC) based method	54
	Stacked de-noising auto encoder (SDNAE) based method	55
	Ensemble learning-based method	56
SBR quantification approach	Cyber-physical resilience (CPR) index	57
		58
		59
	Data-analytic resilience metric	60
		61
	Differential-phasor variance index	62
SBR miscellaneous approach	Weighted mean subsequence reduced-secondary control (WMSR-SC) method	63
	Maximum likelihood estimation method	29
		64

$$\min_{x^i} \|x^i - z^i\|_2^2 \text{ such that, } \|\phi_t x - y_t\|_2^2 \leq \epsilon_t \quad (2)$$

$$d^i = -|x^i|^{p-2} x^i \quad (3)$$

where,  $z$  is the intermediate variable,  $\epsilon_t$  is the error at instant  $t$  with  $\phi_t$  as the orthogonal component for non-convex problem  $y_t$  affected by a malicious attack.  $d^i$  is the direction of search for  $i^{th}$  iteration for the current value of synchrophasor data  $x$ . The simulation results show a higher reconstruction error when the corruption of synchrophasor data is more than 40% in the sample.

In ref. [46] a signature-based PCA is used to examine the malicious synchrophasor measurements. The defined metrics use distinct key features to analyze regular and sub-station data frames. It also summarizes the strength, weaknesses, and interdependencies of this method.

### 5.1.2 | Denial-of-service (DoS) resilient WAMS framework

In ref. [43] DoS resilient framework manages data unavailability due to cyber-attack based on WAMS. Synchrophasor measurements are a series of time-aligned data that avoid delay in assessing cyber-attack conditions and assists in post-event disturbance analysis. The proposed DoS resilient WAMS algorithm uses three modules which are (1) data unavailability detector module (DUDM), (2) root cause analyzer module (RCAM), and (3) DoS mitigation module (DMM) using the k-nearest neighbors (KNNs) approach. The warning mechanism follows counter updation for any new data receipt as shown in Equation (4).

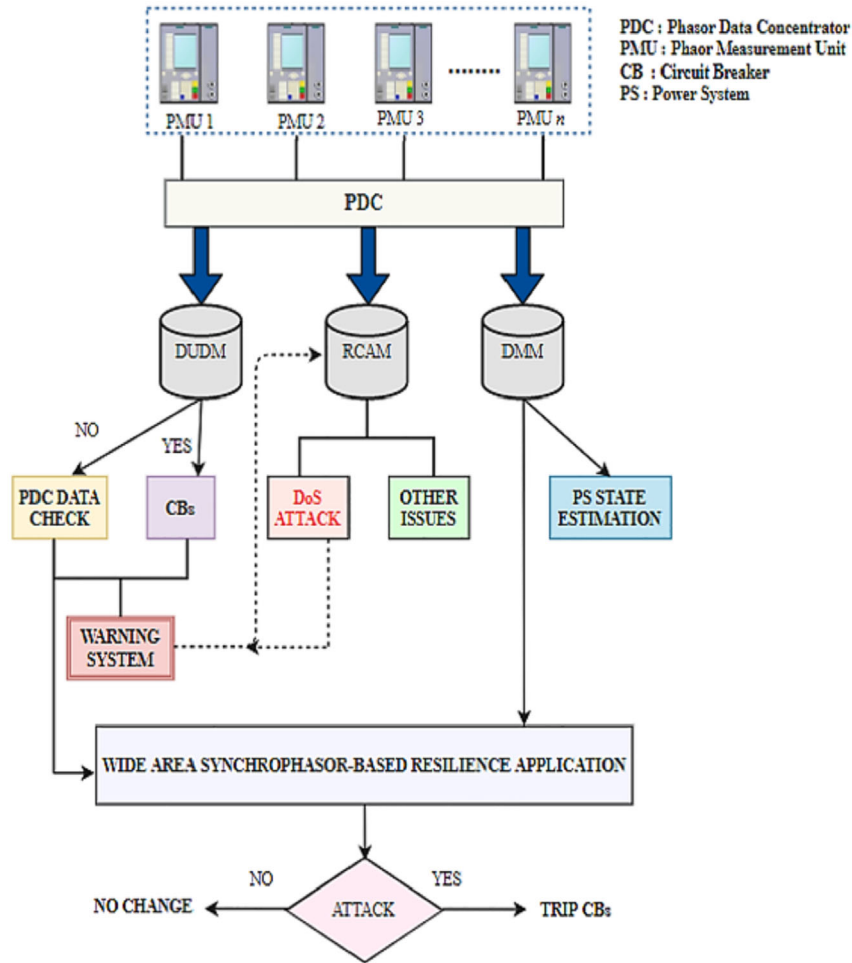


FIGURE 6 Scheme of DoS resilient WAMS framework

$$FR = \begin{cases} fps \pm \delta sec, counter update \\ else, warning \end{cases} \quad (4)$$

$FR$  is the frame rate,  $fps$  is the frame per second, and  $\delta$  is the small deviation. The counter updates upon the receipt of the data stream within the set interval of  $fps \pm \delta$  seconds. Figure 6 represents a resilience framework for synchrophasor based on wide-area monitoring against the DoS attacks. The data flow encountered during a cyber-attack is first accurately identified to estimate its incompleteness. The assessment of the rest available data estimates its closest centroid value. Therefore, DoS attacks are managed effectively. It is a synchrophasor based mitigation strategy without affecting the existing infrastructure.

### 5.1.3 | Distribution system state estimation (SE) framework

A cyber-attack framework using synchrophasor measurement and its SE, is discussed in ref. [44] Existing cyber-attack SE for transmission cannot be effectively extended to the distribution system. So, a distribution system SE framework is required. The relationship between synchrophasor measurements in a general state estimator is represented by Figure 7. Equation (5) expresses the relationship between the estimates and state variables in a classical state estimator. The voltage synchrophasor is the state variable. Considering these parameters, the generic SE formulation takes the form as in Equations (5)–(8).

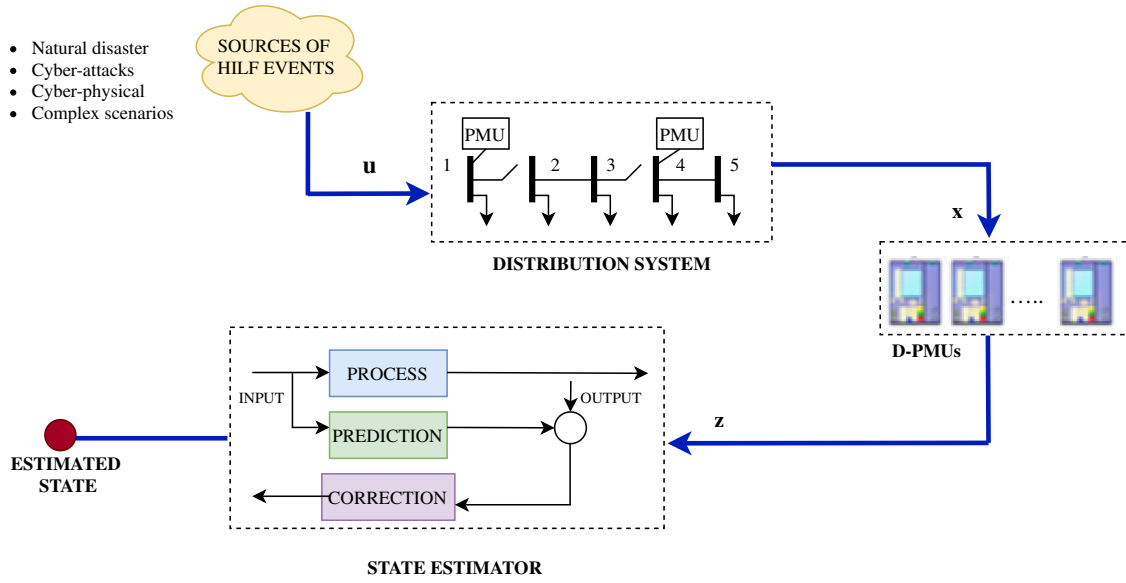


FIGURE 7 Scheme of generic distribution state estimation process

$$z = h(x) + e_{noise} \quad (5)$$

$$\begin{cases} h_{V_{ir}}(x) = z_{V_{ir}}, i \in \Psi_V \\ h_{V_{im}}(x) = z_{V_{im}}, i \in \Psi_V \end{cases} \quad (6)$$

$$\begin{cases} h_{I_{br}}(x) = z_{I_{br}}, i \in \Psi_I \\ h_{I_{bm}}(x) = z_{I_{bm}}, i \in \Psi_I \end{cases} \quad (7)$$

$$\begin{cases} h_{P_i}(x) = z_{P_i}, i \in \Psi_S \\ h_{Q_i}(x) = z_{Q_i}, i \in \Psi_S \end{cases} \quad (8)$$

Where,  $z$  is the measurement vector consisting of PMU data,  $h(x)$  is the measurement function corresponding to  $x$  state vector, the error vector due to noise is represented by  $e_{noise}$ .  $z_{V_{ir}}$  and  $z_{V_{im}}$  are the real and imaginary parts of voltage measurement, respectively,  $z_{I_{br}}$  and  $z_{I_{bm}}$  are the real and imaginary parts of current measurements,  $z_{P_i}$  and  $z_{Q_i}$  are the active and reactive power values. The corresponding measurement functions are given by  $h_{V_{ir}}(x)$ ,  $h_{V_{im}}(x)$ ,  $h_{I_{br}}(x)$ ,  $h_{I_{bm}}(x)$ ,  $h_{P_i}(x)$ , and  $h_{Q_i}(x)$ , respectively.

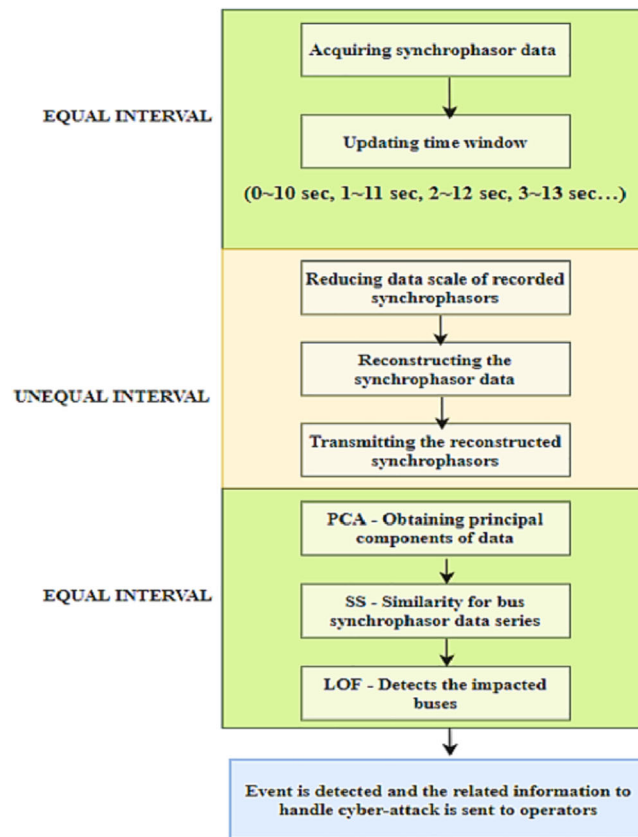
The index of the bus is represented by  $i$  and branches by  $b$ .  $\Psi_V$ ,  $\Psi_I$ , and  $\Psi_S$  refer to the set of buses with voltage, current, and power respectively. Location identification of the spoofed cyber-attack on the network is evaluated by the phase angle  $\theta$  of voltages at bus  $i$  and branch  $b$ , as in Equation (9). Optimization of phase angle narrows the search intervals, as given by Equation (10). The root mean square errors are evaluated at each node to validate the performance, as in Equations (11.a) and (11.b).

$$\theta_{i,b}^{spf} \neq 0 \quad (9)$$

$$\min. \arg J_{corr} = (\theta_1^{spf}, \theta_2^{spf}, \dots, \theta_{PMU_n}^{spf}), \text{ such that, } P1 = \{n | \theta_n^{spf} = \pi\}, P2 = \{n | \theta_n^{spf} \in (0, \pi)\}, P3 = \{n | \theta_1^{spf} \in (-\pi, 0)\} \quad (10)$$

$$(\delta_{V,i}^\varphi)^2 = E \left( \frac{\tilde{V}_i^\varphi - V_i^\varphi}{\tilde{V}_i^P} \right) \quad (11a)$$

FIGURE 8 SS-PCA framework



$$\left(\delta_{\theta,i}^{\varphi}\right)^2 = E\left(\tilde{\theta}_i^{\varphi} - \theta_i^{\varphi}\right) \quad (11b)$$

$P_1$ ,  $P_2$ , and  $P_3$  are the PMU sets. These are predetermined for searching scale purpose forming the argument of the Jacobian matrix for correlation.  $E$  is the expected value of measurements,  $\tilde{V}_i^{\varphi}$  and  $\tilde{\theta}_i^{\varphi}$  represents the true values of voltage measurement and phase angles at the  $i^{th}$  bus,  $V_i^{\varphi}$  and  $\theta_i^{\varphi}$  are the measured values of voltage and phase magnitudes for phase  $\varphi$ . The simulation results show that this hierarchical algorithm is robust against coordinated attacks and multiple spoofing cyber-attacks. Though there is still scope of placing micro-PMUs which can provide a higher degree of accuracy for phase angle error estimation, this resilience-based framework gives good results against spoofing.

#### 5.1.4 | Similarity search-principal component analysis (SS-PCA) framework

In ref. [47] illustration of the use of reduced synchrophasor data mechanism to detect HILF events is proposed. For this purpose, an algorithm consisting of SS and local outlier factor (LOF) concept is applied. SS detects inconsistency in synchrophasor data. LOF uses these fewer synchrophasor data to locate buses affected due to such events. Simulation results show better feasibility of event detection and precise location of impacted buses. Figure 8 represents the step-wise SS and LOF flow diagram. Equal and unequal time frame manages the transmission of reconstructed synchrophasor data and event-oriented algorithm, respectively. PCA removes any chance of multivariate time-series synchrophasor data, followed by SS, and LOF. This real-time application operates every second with a 10 second time window. The overlapped time window (0~10 sec, 1~11 sec, 2~12 sec, 3~13 sec, etc.) increases accuracy. Thus, SA at all times, especially during cyber threat conditions gets enhanced.

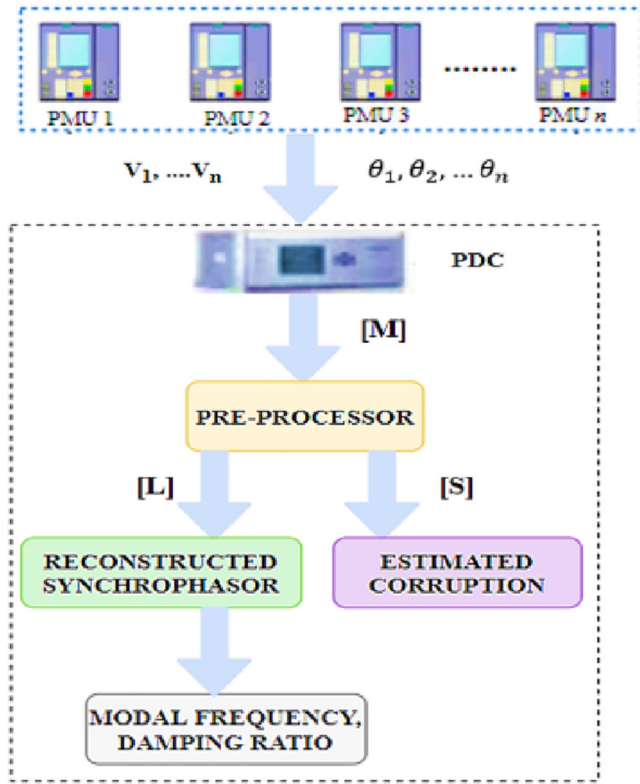


FIGURE 9 Malicious corruption-resilient framework

### 5.1.5 | Augmented Lagrangian multiplier-based (ALM) algorithm

In,<sup>48</sup> resilient wide-area monitoring architecture for malicious data corruption is proposed. It considers three types of cyber-attacks, (1) synchrophasor-data repetition attack, (2) data missing attack, and (3) malicious data injection attack. The augmented Lagrangian function is used to solve the unconstrained optimization problem, as in Equation (12).

$$\text{minimize } g(S, L, Y) = \|L\| + \alpha \|S\|_1 \langle Y, M - L - S \rangle + \frac{\beta}{2} \|M - L - S\|_F^2 \quad (12)$$

Where, data matrix  $M$  represents the summation of low-rank and sparse matrix,  $\alpha$  is a parameter for regularizing smoothness  $L$  and sparseness  $S$ .  $\|\cdot\|$  denotes norm,  $\beta$  is the single regularization parameter,  $L$  is the low-rank matrix, and  $Y$  is the Lagrangian multiplier.

$$\text{Initialization} : S_0 = Y_0 = 0, \beta > 0 \quad (13)$$

$$L_{k+1} = D_{\beta^{-1}}(M - S_k + \beta^{-1}Y_k) \quad (14)$$

$$S_{k+1} = S_{\alpha\beta^{-1}}(M - S_k + \beta^{-1}Y_k) \quad (15)$$

$$Y_{k+1} = Y_k + \beta(M - L_{k+1} - S_{k+1}) \quad (16)$$

Figure 9 represents malicious corruption-resilient framework capable of accurately detecting and timely reconstructing the partially damaged signals. In turn, it leads to an improvement of network resilience.

The matrices  $L_{k+1}$  and  $S_{k+1}$  represent reconstructed data and corruption content at  $(k+1)^{th}$  instant, respectively. Both the low-rank and sparse matrices contain information pointing to the presence of any synchrophasor data inconsistency. The system response vectors are present in the low-rank matrix, while fallacious intrusions are in the sparse matrix. The usefulness of ALM-based algorithm lies in wide-range applicability, less iteration, and hassle-free parameter tuning. Equations (13)–(16) show the initialization and convergence of the algorithm.

## 5.2 | SBR data-driven approach

The data-driven approach provides information from a large set of synchrophasor data streams. Analyzing the data patterns precisely reduces the chance of a massive prolonged impact on the power system. The following sub-sections present a comprehensive discussion of various SBR data-driven techniques used at the distribution level.

### 5.2.1 | Network compensation theorem-based method

In ref. [49] the compensation theorem is adopted to represent the equivalent circuit impacted by abnormal events. It uses the synchrophasor data captured by the micro-PMUs. The current phasors estimate the amount of injection in the network. Bus admittance and voltage at the nodes evaluate the minimization function. Equation (17) represents this minimization function. The phase angle of post-event and pre-event voltage phasors make a  $0^\circ$ , or  $180^\circ$  difference. For event induced equivalent circuit analysis, the phase angle concept is used, as in Equation (18).

$$E_i = \sum_{k=1}^{n-1} \sum_{p=k+1}^n |\Delta V_i^k - \Delta V_i^p| \quad (17)$$

$$\emptyset = \angle Z^{eqv} + \angle \Delta I^{us} \quad (18)$$

Where,  $us$  is upstream synchrophasor data,  $E_i$  is the power factor,  $V$  and  $I$  are voltage and current, index  $k$  is for  $1, 2, \dots, n$  number of micro-PMUs, the index  $i$  is associated with  $1, 2, \dots, m$  number of buses. The compensation theorem in circuit theory identifies the events and enhances SA in distribution systems, thereby extracting only the useful HILF related information.

### 5.2.2 | Hybrid State Estimation (SE) based Method

In ref.[50] the real-time distribution system SE at different time scales is proposed. The data-driven SE comprises deep neural networks (DNNs) and weighted least absolute value (WLAV). It helps in quick tracking of the states of the distribution system. The DNN and WLAV method for estimation uses gradient and topology-based mathematical expression, as in Equations (19)–(21).

$$n = n - \eta \nabla Q_i(n) \quad (19)$$

$$\text{minimize } wv^T |rv| \quad (20)$$

$$\text{such that, } rv = z - h(x) \quad (21)$$

Where,  $n$  stands for the network parameters,  $\eta$  represents the learning rate of DNN,  $\nabla Q_i(n)$  is the gradient of sub-training set  $i$ ,  $wv$  is weight vector,  $rv$  is the residual vector of WLAV,  $h(\cdot)$  represents the measurement function and  $z$  is the hybrid synchrophasor measurement. The WLAV identifies incorrect synchrophasor data, while DNN estimates the topology based state of the system. Therefore, the real-time distribution system monitoring and control improves SA and as a result, improves the resilience of a distribution system against bad data scenarios.

In ref. [51] the sudden undesirable disturbances posing a challenge to the network resilience, using synchrophasor based dynamic SE is addressed. It comprises of three main steps, (1) constant monitoring of the network's most indicative feature, (2) prediction of failures based on constant monitoring, and (3) mitigation of network to prevent further damage.

Figure 10 represents the block diagram of the synchrophasor based dynamic SE. There are three phases, first phase concentrates on model formulation, the second stage uses a prediction algorithm for preliminary data selection and its conditioning that determines system states. The detected error reporting forms the final step. Therefore, the sudden disturbances are systematically handled.

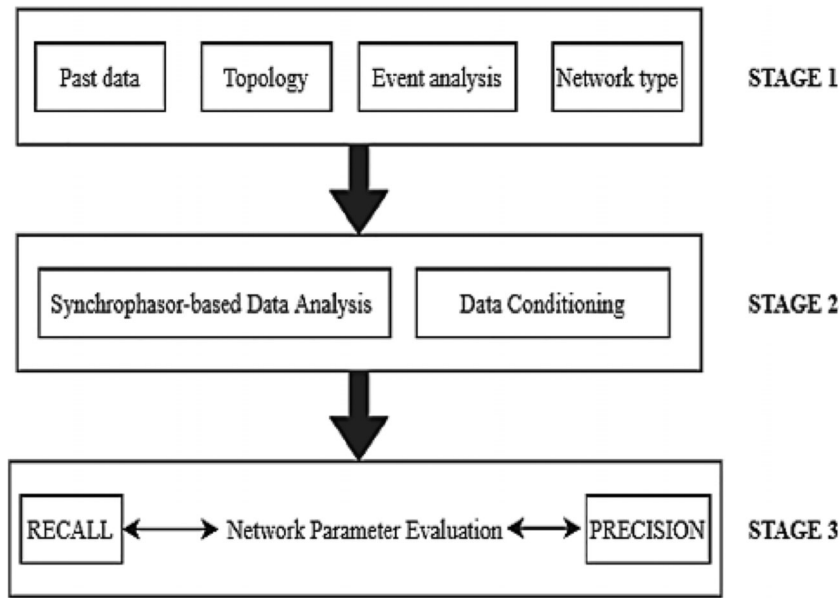


FIGURE 10 Synchrophasor-based dynamic SE

### 5.2.3 | Improved robust-PCA based method

In ref. [52] a stochastic based composite approach for synchrophasor measurement anomaly correction is presented. Application of WAMS aids to accurately recover the transients. Bayesian framework selects the appropriate subspace for post-event synchrophasor measurement recovery. Equation (22) represents the outlier for missing data attacks on the system.

$$x^r = (I - I_{\Omega}I_{\Omega}^T)l^r + I_{\Omega}I_{\Omega}^T x^{r-1} = l^r + \delta^r \quad (22)$$

where the signal corruption is represented as,  $\delta^r = I_{\Omega}I_{\Omega}^T(x^{r-1} - l^r)$

$x^r$  is the synchrophasor measurement vector for sample  $r$ ,  $l^r$  is uncorrupted synchrophasor values for sample  $r$ ,  $\delta^r$  is corrupted vector for sample  $r$ , the index of missing data channels is represented by  $\Omega$ , and the sub-matrix of identity matrix  $I$  is represented by  $I_{\Omega}$ . The output where the probability is one is then chosen for synchrophasor signal recovery. Therefore, this modern composite technique of stochastic sub-space selection and corruption-resilient deviation estimation considers topology changes to extract missing synchrophasors.

### 5.2.4 | Behavioral systems theory-based method

In ref. [53] a behavioral systems theory framework to identify the flaws in data quality due to injected attacks is proposed. It uses synchrophasor voltage, current estimates to capture the inconsistency between past and present measurements. Equations (23)–(25) represents the parametric input, output, and event detection function, respectively.

$$P(u) = \begin{cases} \text{input : } u = V_d \\ V_{node} := \text{col}(V_{I1}, V_{I2}, \dots, V_{In}) \\ I_{node} := \text{col}(I_{I1}, I_{I2}, \dots, I_{In}) \end{cases} \quad (23)$$

$$\text{output : } y := \text{col}(I_d, I_{node}, V_{node}) \quad (24)$$

$$ED(t) = \begin{cases} \text{if } \|M_t - M_{t+1}\|_2 > \xi, \text{ obtain } (p, m) - \text{matrix} \\ \text{else, no event detected} \end{cases} \quad (25)$$

$P(u)$  is the parametric input for input variable  $u$ .  $V_d$ ,  $V_{ln}$ , and  $V_{node}$  are the feeder voltage, load voltage at  $n^{th}$  node and nodal voltage, respectively.  $I_d$ ,  $I_{ln}$ , and  $I_{node}$  are the feeder current, load current at  $n^{th}$  node, and the nodal current, respectively. Modal matrix at  $t$  and  $t+1$  time instants are represented by  $M_t$ , and  $M_{t+1}$ , respectively.  $ED(t)$  is an event detection function with a threshold as  $\xi$ .  $p$  and  $m$  are the nodal indicators of event detection. A possible challenge for this data-driven approach is tuning the threshold with appropriate sensitivity.

### 5.3 | SBR machine-learning (ML) approach

Many of the HILF events cause leads to change in power flow direction. It also causes dips/swells in electric current or voltage measurements. Thus, deploying micro-PMUs aid in the detection and classification capabilities of computer system operators. The advantage lies in the diagnostic capabilities by building consistent synchrophasor data predictions, without much human intervention.

#### 5.3.1 | Bayesian classifier (BC) based method

In ref. [54] the ML method, based on flexible online BC for the detection of cyber-attacks is applied. Laplacian generalized graph matrix (GGL) analyzes the synchrophasor measurements representing the spatiotemporal network patterns. Equation (26) shows the flexible BC objective function, and Equation (27) represents the error.

$$\operatorname{argmax}_{ca \in \Lambda} (A = a \left| \underbrace{\varphi_1^s, \varphi_2^s, \varphi_3^s \dots \varphi_m^s \dots \varphi_{n_s}^s}_{\text{spatial estimation}}, \underbrace{\varphi_1^t, \varphi_2^t, \varphi_3^t \dots \varphi_n^t}_{\text{temporal estimation}} \right|) \quad (26)$$

$$e(h) = E \left[ \int (\hat{P}_h(X|A) - P(X|A))^2 dx \right] \quad (27)$$

Where,  $\varphi_m^s$  and  $\varphi_n^t$  are the spatial and temporal pattern estimations for a total number of  $n_s$  and  $n_t$  synchrophasor measurements.  $\Lambda$  is the number of cyber-attack templates considered, Bayesian condition probability associated with  $A$  variable of cyber-attack instance is represented by  $P$  and denotes as  $P(\cdot)$ ,  $a$  represents attack template corresponding to prior-probability,  $e(h)$  stands for mean integrated square error for  $h$  range,  $X$  is the observed vector of spatiotemporal synchrophasor measurements. Simulation results confirm the ML technique's effectiveness to detect false data injection (FDI) attacks by quantitatively studying these slow changing patterns.

#### 5.3.2 | Stacked de-noising auto encoder (SDNAE) based method

In ref. [55] an ensemble ML and SDNAE method for robust feature extraction and classification of both natural as well as cyber-physical attack is proposed. Feature extraction is a widely-used technique for obtaining attack signatures and dimension reduction. The process consists of SDNAE that acts as a robust feature extraction method and XG Boost algorithm as an ensemble learning-based classifier for the intrusion-detection system, as in Equations (28)–(29).

$$\mathcal{H}_i = f(w_i \mathcal{H}_{i-1} + B_i), i = 1, 2, 3, \dots, 2l - 2 \quad (28)$$

$$\text{where, } \begin{cases} w = [w_1, w_2, w_3, \dots, w_{l-1}] \\ B = [B_1, B_2, B_3, \dots, B_{l-1}] \\ i = 1, 2, 3, \dots, 2l - 2 \end{cases} \quad (29)$$

Where,  $w$  is the weight and  $B$  is the bias for  $i^{th}$  layer,  $\mathcal{H}$  is the hidden layer,  $f(\cdot)$  is the activation function, and network output is determined at  $2l-2$ . The simulation results show that the XG Boost based on the SDNAE can distinguish the regular network functioning from attack-events with higher accuracy.

### 5.3.3 | Ensemble Learning based method

In ref. [56] the detection of FDI attacks and its analysis for stable cyber-physical operation is explored. During such an attack, the distribution system stability gets hampered. The ensemble classifier constructs the FDI attack affected synchrophasor data automatically and accurately. Equations (30)–(33) represents the FDI attack detection model. It classifies the input synchrophasor data and the related detection results.

$$Y_i = \begin{cases} 1, & \text{FDI - attack} \\ 0, & \text{else} \end{cases} \quad (30)$$

$$D = \begin{pmatrix} D_{11} & \cdots & D_{1n} \\ \vdots & \ddots & \vdots \\ D_{j1} & \cdots & D_{jn} \end{pmatrix} \quad (31)$$

$$Y_j = \begin{cases} 0, & \text{no attack detected} \\ 1, & \text{normal system fault} \\ 2, & \text{type 1 FDI - attack : synchrophasor - tampering} \\ 3, & \text{type 2 FDI - attack : synchrophasor - tampering} \\ 4, & \text{type 3 FDI - attack : PMU settings - tampering} \end{cases} \quad (32)$$

$$Y = \{Y_1, Y_2, \dots, Y_j\}, \text{ for } i \text{ number of samples in the synchrophasor data} \quad (33)$$

$D$  represents the original synchrophasor data set for  $j^{\text{th}}$  samples, with dimension  $n$ . The simulation results show that it can detect different FDI attacks, even on small data.

## 5.4 | SBR quantification approach

The synchrophasor data of voltage/current changes, failure distribution, reliability, and stability can be measured to estimate the degree of performance losses. Based on these parameters, performance during normal condition and network loss under hazardous scenarios are quantified. This section explores the different quantification techniques of SBR.

### 5.4.1 | Cyber-physical resilience (CPR) Index

In ref. [57] metrics for cyber and physical domain in response to abnormalities in the cyber-physical system are defined. Equations (34)–(35) represents the CPR index and related cost constraints.

$$CPR_s = V^{op}_s \quad (34)$$

$$U = \max \int_0^\infty f(t)^T H f(t) + u(t) G u(t) dt \quad (35)$$

Where,  $s$  is the number of states, and  $V^{op}_s$  is the optimal value corresponding to state  $s$ ,  $U$  is the cost of recovery,  $u(t)$  is the input,  $f(T)$  is the set of states that are reachable by the adversary within time  $T$ .  $H$  and  $G$  represent matrices describing the cost of deviating from the zero state and the cost of control, respectively. The states can be evaluated by the modified Viterbi method to assess data uncertainties to quantify mismatch.<sup>57</sup> This SSL approach is an information-assessment technique to determine potential adverse events that can affect the system.<sup>58</sup>

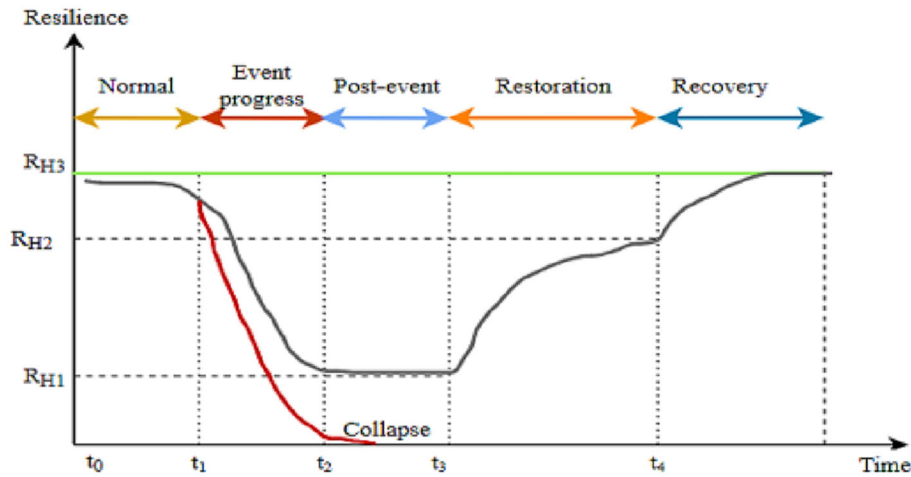


FIGURE 11 Resilience graph for distribution system

#### 5.4.2 | Data-analytic metric using resilience curve

In ref. [60] a series of not so common disturbances that tend to disrupt the normal functioning of the distribution system are addressed using resilience curve.

Figure 11 represents data-analytic metrics based on the resilience curve. The different phases such as event progress, post-event, restoration, and recovery corresponds to phase-wise transition of distribution system. It helps to analyze the resilience requirements and aims at attaining specific performance level, that ultimately prevents total system collapse. The simulation results show that DERs have the inherent capability to enhance resilience by compensating for a loss of 1,800 kWh for a 13-bus distribution system.

In this graph,  $R$  represents the generic-resilience metric,  $R_3$  is the operation mode for ideal scenarios and  $R$  is the post-event operation mode,  $t_1$  and  $t_4$  represent the ideal restoration time and post-event restoration time horizon, respectively. Equation (36) represents a generic resilience framework considering the predisturbance phase to the post-restoration stage.

$$R = \int_{t_1}^{t_4} [R_3(t) - R(t)] dt \quad (36)$$

In ref. [61] a weighted mean approach for secure mitigation against intrusion attack is proposed. The error in micro-PMU data is quantified using the intrusion index. Equations (37)–(38) represents voltage synchrophasor estimates and the percentage of corruption in data.

$$M_t = U_t + S_t \quad (37)$$

$$C\% = \begin{cases} 0, & (\|S_t\|_0 = 0) \\ 20, & (\|S_t\|_0 = 2S_t) \\ 100, & (\|S_t\|_0 = 1) \end{cases} \quad (38)$$

Where,  $M_t$  is the time-sequence measurement vector consisting of voltage synchrophasors,  $S_t$  is the sparse vector,  $U_t$  is the uncorrupted past measurements vector,  $C\%$  represents the percentage of corruption in data. Evaluation of corruption percentage mitigates the intrusion by deploying the required amount of measures to recover the corrupted PMU measurements.

### 5.4.3 | Differential-phasor variance Index

In ref. [62] the evaluation of synchrophasor data inconsistency using statistical measure is explained. Variance of voltage synchrophasors at the impacted bus to rest buses is  $\Delta V$ . The identification of the buses based on the voltage measurement values  $S$  (it's cardinality  $s$ ) using  $j$  number of PMUs, is as in Equation (39). As an alternative, the cyber-attack can also be detected by checking the variance compared to the threshold value  $\partial$ , as in Equation (40).

$$\text{var}(\Delta V_j)_S = \frac{1}{s} \sum_{i=1}^s (\Delta V_j^s)^2 - \left( \frac{1}{s} \sum_{i=1}^s \Delta V_j^s \right)^2 \quad (39)$$

$$\prod (\text{var} \{ \Delta V_j \}) > \partial \quad (40)$$

The exact location of impacted micro-PMUs can be determined by this method. The added advantage is that prior knowledge about PMU numbers and site information is not required.

## 5.5 | SBR miscellaneous approach

This section addresses resilience, along with integrity, availability, and security functionalities of the distribution network. It is a combination of network behavior, boundary conditions, protective actions, and DER-related decisions.

### 5.5.1 | Weighted mean subsequence reduced-secondary control (WMSR-SC) method

In ref. [63] security against cyber-attacks using secondary control process by deploying PMU and its communication link is detailed. The PMU based communication link quality with respect to the power angles  $\delta$  between bus  $i$  and  $j$  for power angle thresholds  $P_1$  and  $P_2$  is represented as in Equation (41).

$$C_{ij} = \begin{cases} C_{max}, & |\delta_i - \delta_j| < P_1 \\ 0, & |\delta_i - \delta_j| \geq P_2 \\ C_{max} e^{\left( \frac{\alpha (|\delta_i - \delta_j - P_1|)}{P_2 - P_1} \right)}, & \text{else} \end{cases} \quad (41)$$

Where,  $\alpha$  is the design parameter. The system's health monitoring is estimated from the closeness of power angles. A less power angle gap threshold  $P_1$  denotes stable system frequency.  $C_{max}$  represents the maximum value of data packet transmission rate within the network.

### 5.5.2 | Maximum likelihood estimation method

The technique for maximum likelihood node for anomaly detection, framed in ref. [29] is a proactive method. It uses processed data to figure out a satisfactory response. The main principle is that the synchrophasor located at/near the adverse event experiences vast variation in measurement than the farther ones. Equation (42) represents the simplified 2-node instantaneous power flow.

$$P_{AB} = \frac{|V_A|^2 + |V_B|^2}{|Z|} \angle \alpha - \left[ 2 \left( \frac{|V_A| |V_B|}{|Z|} \right)^2 \cos(2\delta + 1) \right]^{\frac{1}{2}} \angle \alpha \quad (42)$$

Equation (43) classifies impacted feeders based on bus angle change.

$$\frac{\Delta \delta}{\Delta t} = \frac{\delta_{w+1} - \delta_w}{360^\circ \times w} \quad (43)$$

$\delta$  represents the resultant angle due to the two voltage vectors,  $Z\angle\alpha$  is sectional impedance,  $|V_A|$  and  $|V_B|$  are the voltage of buses as obtained from D-PMUs. This method of anomaly classification based on the bus angle helps to identify the critical nodes. It reconfigures the network in a manner that the angle difference becomes a near-zero value. Thus, the resilience of a distribution system improves by timely shifting the critical loads during unfavorable events.

In ref. [64] a comprehensive assessment of synchrophasor measurement uncertainties and related operating conditions are analyzed. Equations (44)–(45) represents the magnitude and phase of random noise added to  $N$  sets of measurement. Its total vector error is as in Equations (46)–(47).

$$\Delta m N(0, err_m/3), X_m^M = X_m^T + \Delta m \quad (44)$$

$$\Delta p N(0, err_p/3), X_p^M = X_p^T + \Delta p \quad (45)$$

$$err_m = f(TVE)|_{err_p=0} \quad (46)$$

$$err_p = f(TVE)|_{err_m=0} \quad (47)$$

Where, the magnitude and phase for noise are  $\Delta m$  and  $\Delta p$  respectively.  $X$  is a generic quantity and  $T$  is for true quantity. Magnitude and phase errors are represented by  $err_m$  and  $err_p$  respectively.

Figure 12 provides a percentage-wise categorization of various methods that are used for SBR applications. It can be deduced that the SBR model based and SBR quantification approach can precisely estimate the change in performance due to HILF disturbances, and are widely implemented. The uncertainty based operating conditions during HILF events is estimated using errors of synchrophasor measurements to accurately predict the restorative actions to be considered for SBR.

## 6 | SBR APPLICATIONS

This section outlines various applications of SBR considering the available literature. It classifies the application to obtain the most suitable SBR, under a given set of available resources. These applications are voltage stability and oscillation monitoring; disruption detection and mitigation; combined infrastructural and operational control; and other abnormal conditions.<sup>65–68</sup> Figure 13 represents SBR applications responsible for protecting the distribution system degradation due to the HILF events. Table 7 enlists the details of SBR applications in the distribution system for different HILF scenarios.

Figure 14 shows the percentage of previous research works for SBR applications.

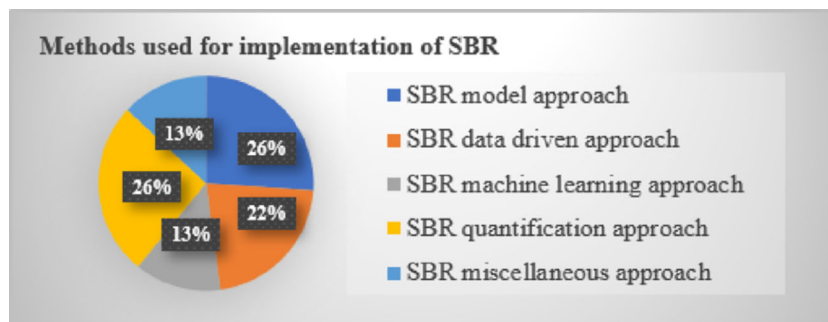


FIGURE 12 Percentage-wise details of methods used for SBR implementation

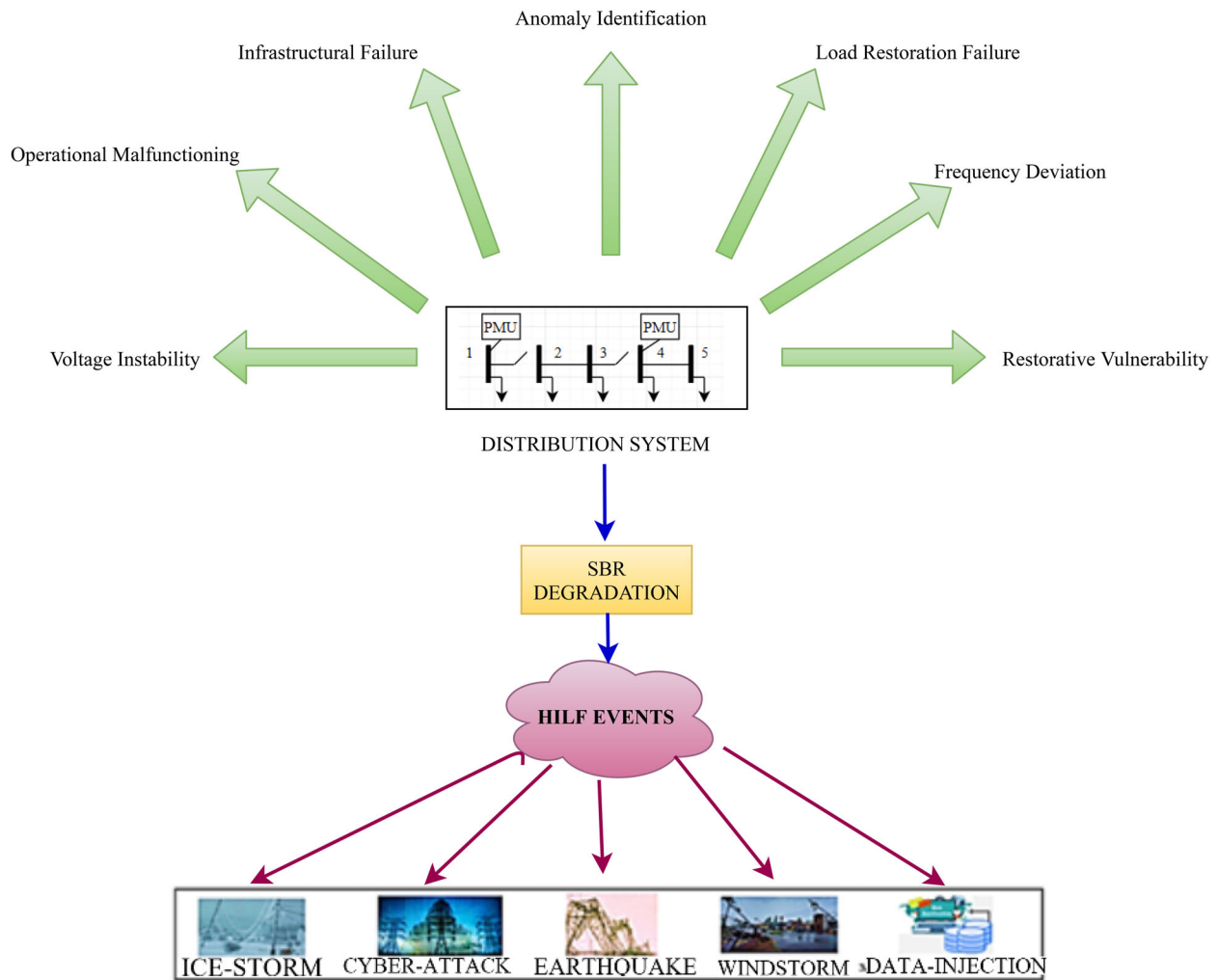


FIGURE 13 Representation of distribution system degradation and related SBR applications

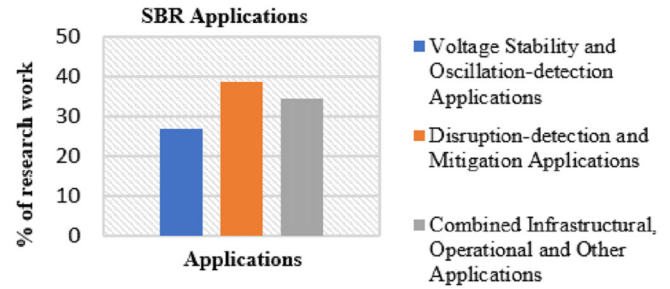
SBR applications	References	SBR applications	References
Voltage instability	43,65,69,70	Oscillation issues	65,71,72,73
Disruption detection	74,50,51,53,75	Operational malfunctioning	50,55,57,24,76
Mitigation issues	42,44,46,47,55,77	Load restoration failure	69,29
Infrastructural failure	45,74,78,79,21,80	Anomaly identification	49,53,29,79
Frequency deviation	60,59,66	Restorative vulnerability	68,81,75,78

TABLE 7 Applications of SBR in distribution system for HILF events

## 6.1 | Voltage stability and oscillation applications

This sub-section deals with the SBR application-related literature that predicts system oscillation and enhances voltage stability. Comparison of past and present voltage and current synchrophasor datasets can identify such abnormalities.<sup>44</sup> The variance of time sequence voltage synchrophasor from its threshold value gives the micro-PMU data inconsistency.<sup>49,53</sup> The synchrophasors near to the HILF location experience a larger deviation in measurements. It checks anomalies to estimate the percentage of corrupted data.<sup>29,61-63</sup> High probability of information distortion is monitored by oscillation detection at each node. It helps in the supervision of network hijacking scenarios.<sup>65</sup> The real-time voltage measurement is integral to all types of resilience enhancement against cyber-physical, cyber, and network

FIGURE 14 Percentage wise details of research work in SBR applications for the distribution system



malfunction.<sup>66</sup> To dynamically track cyber anomalies, nonlinear SE is commonly deployed.<sup>67</sup> Distributed generation (DG) aids in a stable and reliable benefit for intermittent voltage and frequency control. For windspeed disturbance, the kinetic energy of a rotating mass determines the maximum operating point. Beyond this, resilience measures are applied because the network reaches its maximum controlled efficiency.<sup>76,82</sup>

In ref. [72] a recursive method calculates and updates the threshold settings for deviations in synchrophasor data. This leads to a reduction in the false alarm rate during abnormal situations. It uses a fast local synchrophasor information recording and processing method. The raw synchrophasor data are represented in the form of a matrix, with  $a$  number of samples,  $b$  variables, and  $m$  number of principal components. Equation (48) shows this matrix representation, and Equation (49) gives its score by the Hotelling's formula. Figure 15 represents a robust PCA framework to monitor the synchrophasor based data-driven approach applied for resilience enhancement by islanding.

$$\mathbb{Q} = S\mathcal{L}^T + \mathfrak{R} \quad (48)$$

$$S_i^2 = \mathbb{Q}_i \ell Y^{-1} \ell^T \mathbb{Q}_i^T \quad (49)$$

Here,  $\mathbb{Q}$  and  $\mathfrak{R}$  are the observation and residual matrix,  $S$  and  $\mathcal{L}$  are the score and load vectors, respectively.

Where,  $S_i^2$  is the  $i^{\text{th}}$  row of the Hotelling's principal component analysis statistic,  $Y$  is the diagonal matrix containing  $k$  eigenvalues.  $\ell$  is the score corresponding to  $i^{\text{th}}$  row.

In ref. [84] voltage and frequency synchrophasors are correlated, with the network's active and reactive power consumed by the load. Equations (50)–(51) represents the basic formulations for threshold  $Th$  estimation in these types of detectors. The ZIP-static load model, with constant impedance ( $Z$ ), current ( $I$ ), and power ( $P$ ), is as in Equation (52).

$$Line_{regression} = \beta y + \alpha \quad (50)$$

$$Th = \begin{cases} Th_{high} = \beta y + \alpha + p * dev \\ Th_{low} = \beta y + \alpha - p * dev \end{cases} \quad (51)$$

$$\mathbf{P} = Z_p V^2 + I_p V + \mathbf{P}_p \quad (52)$$

Where,  $\beta$  represents the slope of the regression line, the value of intercept is given by  $\alpha$  and the closest point on the line from the actual data is shown by  $y$  in the equation,  $p$  is the count of standard deviations and  $dev$  represents root-mean-square of  $y$ -distance from the given regression line.  $P$  and  $V$  are the active power and voltage in per unit with sub-script  $p$  denoting the positive component.

In ref. [73] the synchrophasor data for oscillation detection, SE, and other remedial actions are explored. For a fast extreme event diagnosis, ensemble based learning technique is used. Figure 16 represents the anomaly detection process based on outlier identification and ensemble technique. It provides a trigger for further classification into bad data or events. The anomaly score of synchrophasor data is based on the aggregate score computed by the detector.

Figure 17 is a graphical statistic of previous research works on voltage stability and oscillation applications for SBR. The increase in frequency poses a challenge to the system's voltage and oscillation margin. An integrated solution based on grid modernization is used to achieve satisfactory results and SA improvement, and a greater chance of survivability from system damage.

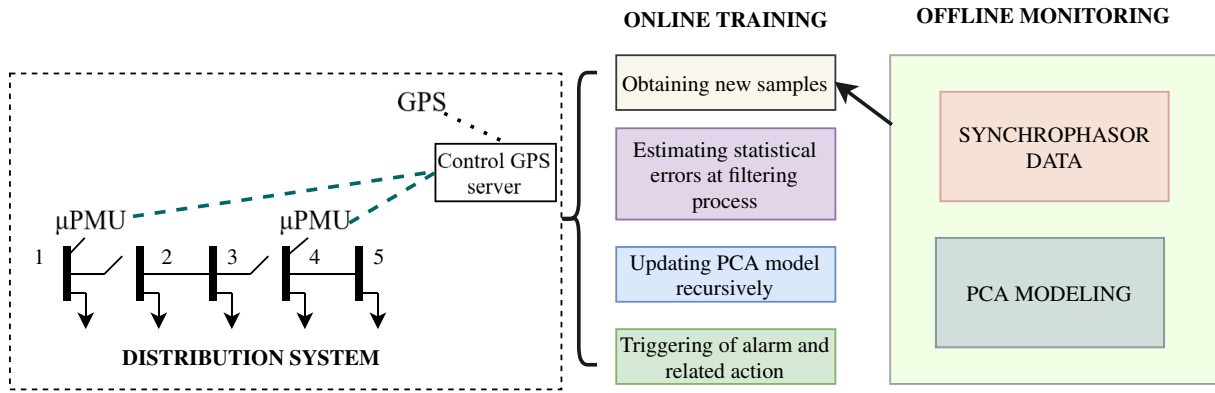


FIGURE 15 Scheme of PCA approach<sup>83</sup>

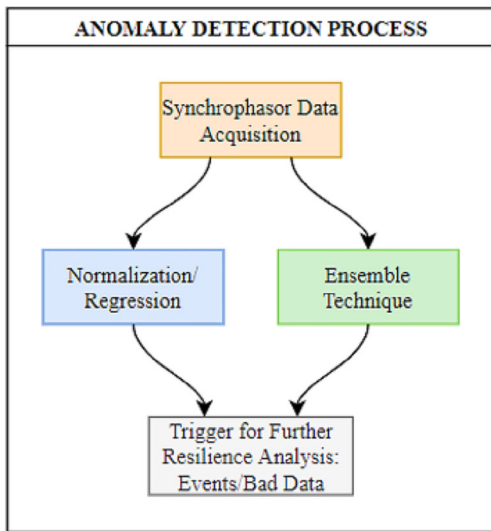


FIGURE 16 Anomaly detection process

## 6.2 | Disruption detection and mitigation issues

This sub-section outlines applied work regarding the improvement of distribution system disruption detection and its appropriate mitigation measures. The wide-area resilience framework focuses on synchrophasor data based mitigation strategies with less impact on the existing infrastructure.<sup>42,44</sup> Accurate detection and recovery of synchrophasor data from the corrupted measurements prevent further degradation.<sup>47,48</sup> Monitoring its most indicative feature aids mitigation during intrusion and adverse weather.<sup>51,52</sup> The classification of HILF events into natural and cyber-oriented events help in robust feature extraction.<sup>54,56</sup> The micro-PMU provides exactness in the estimation of restoration and thereby improves SA for post-HILF condition.<sup>68</sup>

In ref. [81] an integrated resilience framework for preventive and emergency response is proposed. The SA based resilience corresponds to response strategies based on outage prediction and load shedding of the distribution system. Equation (53) represents an objective function for power optimization using this integrated framework. Equations (54)–(55) is the uncertainty modeling of distribution lines due to stormy weather. Equation (56) is the power optimization function during an emergency. Figure 18 represents the decomposition strategy based on an integrated response framework for resilience based on preventive measures, emergency response, and above all SA.

$$\max. \sum_{d \in \mathcal{N}} \phi_{d,shed}^{em} \tag{53}$$

FIGURE 17 Graphical representation of % of SBR explicit/implicit researches on voltage stability and oscillation applications

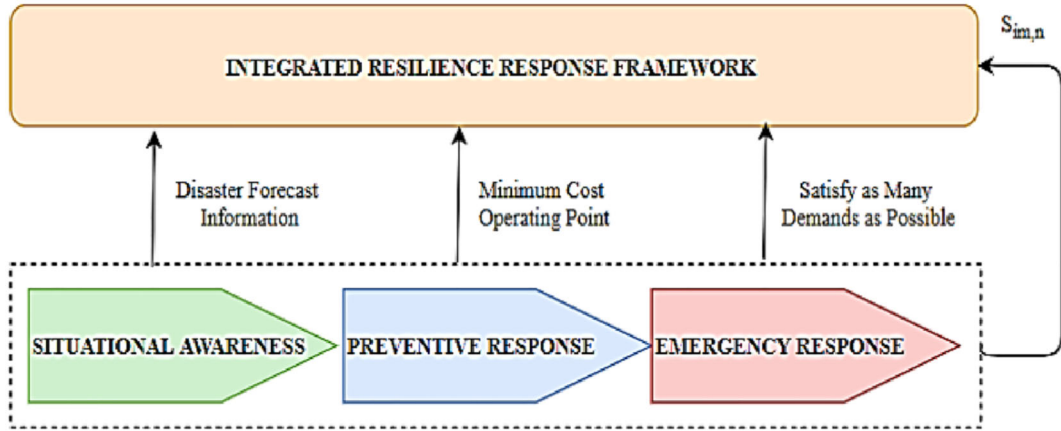
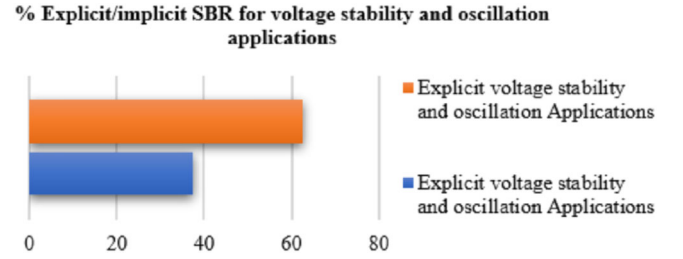


FIGURE 18 Decomposition of integrated response framework for resilience

$$\sum_{(m,n) \in \ell} (1 - \mathbb{N}_{m,n}^b) \leq \mathcal{L}^b \quad (54)$$

$$\begin{cases} \mathbb{N}_{m,n}^b = 0, \text{line damaged} \\ \mathbb{N}_{m,n}^b = 1, \text{line not - damaged} \end{cases} \quad (55)$$

$$\min. \sum_{d \in \aleph} \mathcal{G}_{d,shed}^{em} \quad (56)$$

$\mathcal{G}_{d,shed}^{em}$  is emergency state power drop of a load,  $\aleph$  is total load. The maximum number of lines damaged is represented by  $\mathcal{L}^b$ .  $\mathbb{N}_{m,n}^b$  shows that line  $(m,n)$  out of total  $\ell$  lines may be damaged under windstorm. In ref. [69] a two-stage decision for optimal load restoration, using the mixed-integer method is determined. Equations (57)–(63) represents objective functions to satisfy the voltage, current, power, restored loads based on operational constraints, respectively.

$$\max f(\mathcal{L}) = \sum_{j \in \mathcal{L}} w_j \mathcal{L}_j, \text{ with, } \mathcal{L}_j \in \{0, 1\}, \forall j \in \mathcal{L} \quad (57)$$

$$a_{j,k}, b_{j,k}, b_{k,j} \in \{0, 1\}, \text{ for } (j,k) \in \gamma', V_k^\varphi \in \mathcal{C}, p_j^\varphi, q_j^\varphi \in \mathcal{R}^+ \text{ for } j \in \aleph, \varphi \in \alpha_j \text{ and } I_k^\varphi \in \mathcal{C}, \text{ for } (j,k) \in \gamma, \varphi \in \alpha_j \quad (58)$$

$$\text{Such that } \begin{cases} p_j^\varphi + j q_j^\varphi = V_k^\varphi \sum_{m \in \sigma_j} I_{kj}^\varphi \mathcal{H} \\ I_{kj}^\varphi = \sum_{r \in \gamma_j} Y_{kj}^\varphi r (V_j^\varphi - V_k^\varphi) \end{cases} \quad (59)$$

$$\begin{cases} 0 \leq \sum_{\varphi: \varphi \in \alpha_j} (p_j^\varphi + \mathcal{L}_j p_{load,j}^\varphi) \leq P_{rate,j} \\ 0 \leq \sum_{\varphi: \varphi \in \alpha_j} (q_j^\varphi + \mathcal{L}_j q_{load,j}^\varphi) \leq Q_{rate,j} \end{cases} \quad (60)$$

$$\begin{cases} p_j^\varphi = -\mathcal{L}_j p_{load,j}^\varphi \\ q_j^\varphi = -\mathcal{L}_j q_{load,j}^\varphi \end{cases} \quad (61)$$

$$V_{k,min}^\varphi = \leq |V_k^\varphi| \leq V_{k,max}^\varphi \text{ for } j \in \mathbb{N}, \varphi \in \alpha_j \quad (62)$$

$$|I_{k,j}^\varphi| \leq I_{k,j,max}^\varphi, \text{ for } (j,k) \in \gamma, \varphi \in \alpha_j \quad (63)$$

Where,  $\mathbb{C}$  is the complex number set and  $\mathfrak{R}^+$  is the set of positive real numbers. For load  $j$ ,  $\mathcal{L}_j$  is the critical load restoration solution, for the  $j^{\text{th}}$  load  $w_j$  is the weight factor, and for lines  $(j,k)$ ,  $a_{j,k}, b_{j,k}, b_{k,j}$  are the selected line status to be energized.  $V_k^\varphi$  and  $I_k^\varphi$  are the voltage and current synchrophasors for phase  $\varphi$  at bus  $j$ ,  $\sigma_j$  represents the adjacent buses with phase  $\alpha_j$ ,  $Y_{k,j}^\varphi$  is the admittance between buses  $k$  and  $j$  with a phase difference  $\varphi$ . The total real and reactive power of load at bus  $j$  is represented by  $p_j^\varphi$  and  $q_j^\varphi$ , respectively. The objective of these equations is to maximize the restored loads based on operational constraints, as in Equation (57). The unbalanced three-phase power flow applying Kirchhoff's law is indicated by Equation (58). The objective function also considers Ohm's law. The bus injection based on power constraints is indicated by Equations (59)-(63). At times, if the intensity of system damage is large, then the load recovery is postponed to satisfy the network's minimum operational constraints.<sup>85</sup>

Building small scenarios of wind energy farm output using synchrophasor measurements at each instant is detailed in ref. [75] Equation (64) gives a discrete solution for the wind farm restoration scenarios. The value of 1 means that the wind farm is restored safely at the opportune time  $t$ .

$$f = F(P_{wind\ farm}, t) \quad (64)$$

$P_{wind\ farm}$  represents output power of the wind farm, and time  $t$  denotes the mitigation time.

SBR enhances the detection of HILF events and prevents further degradation. WAMS based on data synchronization handles the real-time monitoring and incident analysis for emergency control.<sup>77,86</sup> A sectionalisation method also accelerates network mitigation. Small integer linear programming (SILP) model with an improved PMU placement algorithm is used for this.<sup>78,80</sup>

All the above-discussed SBR applications improve distribution system resilience. It coordinates real-time measurements with the different optimization strategies. Therefore, detection and analysis of abnormal events at exact instance enhances SA.

### 6.3 | Combined infrastructural, operational, and other applications

SBR reinforces the infrastructural strength and operational performance of a system. The combined monitoring of both these aspects gives a complete picture of the network.<sup>46,50</sup> Quantifying these interdependent synchrophasor data gives possible disruption causes due to HILF events.<sup>55,57</sup> Also, intelligent restoration with the help of new technologies increases observability.<sup>59,60</sup> Other applications of SBR includes improved emergency response due to better communication channels and topology monitoring at all time scales.

In ref. [71] WAMS monitors the distribution system operational parameters to check the restored system till it becomes stable. The method proposed in ref. [71] is extended to estimate resilience in ref. [24] Coordinated resilience improvement technique monitors and controls the time dependent service interruptions. In ref.[74] a resilience oriented look ahead method is proposed. The disturbance due to HILF impact is divided into a sequence of periods. It comprises of three steps that are feeder selection, optimal usage of DERs, and operational efficiency. The objective function of this

proposed method aims at minimizing the mismatch between node voltages and the real power of DGs. Equations (65)–(66) represents the optimization function for obtaining a target resilience.

$$\min \sum_{g=1}^G w_g (\bar{P}_g - P_{g,k})^2 + \sum_{u=1}^U w_u (v_u^{set} - v_u)^2 \quad (65)$$

$$\max \sum_{d=1}^D \sum_{t=k}^K c_d x_{d,t} T_{int} \quad (66)$$

Where,  $\bar{P}_g$  represents real power of the DGs, the predecision variable on real power is  $P_{g,k}$ ,  $k$  is the first length of time considered,  $w_g$  and  $w_u$  are weighted coefficients,  $v_u$  and  $v_u^{set}$  are the node voltage and their target values respectively, the sum of priorities of  $d$  loads in service are  $c_d$ ,  $D$  is total loads in service, the status of load is  $x_{d,t}$  in each time duration  $T_{int}$ . By appropriate control techniques, the adverse impact of DGs on the resilience based operation after a major disaster can be determined.

WAMS captures the operational status of the system.<sup>78</sup> This information is capable of maintaining the active power balance and related operational constraints. Classifying events based on mismatch of operational parameters are discussed in ref. [79] In ref. [21] the benefits of quantification of synchrophasor based resilience are discussed. The overall topological resilience metric  $\mathcal{R}_T$ , in terms of its voltage, under a certain type of reconfiguration  $\mathfrak{G}(k, i)'$  for the distribution system is given by Equation (67).

$$\mathcal{R}_T = \sum_{i=1}^N V_i \mathfrak{G}(k, i)' \quad (67)$$

The metric as discussed effectively captures the distribution system's preparedness to handle the impact of extreme events. Therefore, a multivariate analysis of resilience yields better results for future distribution systems.<sup>80</sup> Equation (68) quantifies this multi-criteria analysis, that is evaluated using graph theory and the Choquet integral.

$$CI_\rho(f) = \int f d\rho = \sum_{i=1}^n (f(y_i) - f(y_{i-1})) \rho(\Lambda_i) \quad (68)$$

$\rho$  is the measure on which Choquet integral ( $CI$ ) is defined on a set of criteria  $Y = [y_1, y_2, \dots, y_n]$ , the  $CI$  of a function  $f: Y \rightarrow R+$ ,  $\Lambda_i$  represents nonempty sets for different alternatives.

Switching operation reduces the probability of more failures in the network. During service restoration process, it minimizes the disruption time of loads. In ref. [70] improving SA is recognized as a catalyst for providing information about switching tasks and related grid operations during event propagation. Figure 19 represents the sequence-wise phases of resilience.

In ref. [29] proactive measures of resilience using D-PMUs are analyzed. In ref. [29] recursive principal component analysis (RPCA) dealing with the event-based transients is proposed. It detects any islanding in the system. ALDC algorithm is implemented across the PMUs to segregate all data whose error exceeds a predefined threshold level.

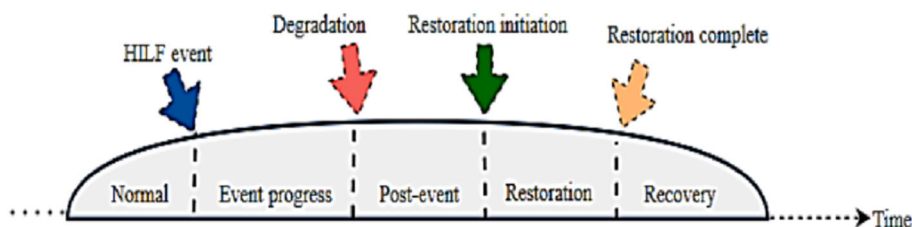


FIGURE 19 Evolution of need for operational and infrastructural resilience

Thus, the application of SBR enables infrastructure, operational, and its combined benefits on the system's performance. Its quantification based on control, monitoring, reconfiguration, and proactive techniques averts any impending HILF conditions.

## 7 | COMPARATIVE ASSESSMENT OF SBR

This section presents an elaborate comparison of SBR literature proposed by numerous researchers. It contrasts the attributes of SBR, its type i.e. response-based (post-incident planning) or event-based (incident-focussed), its features, network parameters, attack type, limitations, and HILF event stage. The applications of SBR, methods used for its implementation, and details of the SBR approaches are also examined for correlation. Table 8 presents a comprehensive comparison of the various SBR approaches based on the above points. From Table 8, it is evident that a major portion of the SBR assessment methods are event-centered. It means that the synchrophasor data will be used mainly for after-math resilience analysis of the distribution system according to the HILF intensity. The network parameters are contrasted based on the impact on DGs, network configuration, and topology identification. The SBR model based approach is used to analyze almost all types of attacks such as DoS, spoofing, data corruption, and substation attack. Topology identification addresses malfunction of location due to voltage instability and oscillation issues. It examines post-mortem analysis for disruption detection and mitigation difficulty. Template/data set formation is probed using topology for combined infrastructure, operational and other anomaly issues. Most of the SBR methods are tested on the normal configuration of the network. The utilization of SBR methods depends on issues encountered by the network and SBR type suitable under HILF scenarios.

Thus, based on available literature, the following deductions may be drawn:

Figure 20 illustrates percentage-wise different issues of SBR pertaining to existing literature. It can be deduced from the pie chart that the SBR approach is mainly implemented for disruption detection and mitigation difficulties in the system.

Table 9 distinguishes the SBR methods based on accuracy, data sample efficiency, simulation results, merits, and demerits. Based on accuracy, it is found that the SBR data-driven and SBR machine learning approach captures fast system variations for resilience estimation. It is observed that the machine learning approach shows greater efficiency for results related to detection and classification, as in ref. [56] However, this approach is dependent on datasets and simulated test-beds may not always be available or at times there may be a lack of expert knowledge. The sample efficiency of the SBR data-driven method is high but also sensitive to bad data. In ref. [54] the synchrophasor bad data related to spatial and temporal characteristics are estimated as a nonlinear function of its multivariate resilience nature. SBR miscellaneous method is dependent on a control and communication system for a reliable simulation result. Very few attempts to apply the machine learning approach for SBR can be seen in the literatures. In refs. [55,56] the classification of HILF events majorly focuses on system resilience by analyzing diversified synchrophasor measurements separately. It can sometimes lead to lengthy procedures for evaluating resilience using the SBR machine learning method due to a large number of synchrophasor data required for preprocessing. Based on SBR merits, the SBR quantification method does not require data modeling techniques. The knowledge of features based on data accuracy, sample efficiency, simulation results, merits, and demerits enables appropriate selection of methods. It addresses some of the challenges that can arise during the practical application of SBR methods to the distribution system for HILF scenarios.

## 8 | FUTURE RESEARCH PERSPECTIVES

As per the survey, the various implementation techniques, framework, classification, and impact of SBR on the power system are presented. It is evident from the existing literature that no universally accepted parameter is available for a holistic SBR framework.<sup>92-94</sup> The modern power system has shown signs of technological advancements along with greater inclusion of DERs that may lead to technical and economic challenges for the aging distribution system.<sup>95-97</sup> In this section, few perspectives for applying SBR in future are as follows:

- i. The distribution system is evolving in nature. The conventional distribution system may have difficulty in handling the changing customer demands and increase in extreme events. So, in the future, a set of practical guidelines to overcome the geographical limitations to track distribution line status using unmanned aerial vehicle is needed.<sup>98</sup>

TABLE 8 Detailed comparison of SBR in distribution system for HILF scenarios

Network parameters							HILF event stage		
Issues	Ref	SBR Method used	SBR type	Methodology features	Impact on DG	System/ Configu-ration	Topology identification	Limitations	Based on attack type
Voltage instability and oscillation	44	SBR model based	EC-SBR	Multiple coordinated spoofing attacks transformed into single event	No effect of DG penetration due to high accuracy algorithm	IEEE 34, 123-bus/normal config.	Phase shifts are obtained based on network's topology	Micro-PMUs with higher measurement accuracy could give better result	Spoofing attack
	49	SBR data driven	RC-SBR	Application of circuit theory concept using WAMS	DG bus sensitivity is correctly obtained	IEEE 123-bus	Topology aids in device malfunction location	At least two micro-PMUs are required	PMU data corruption
	53	SBR data driven	EC-SBR	Synchrophasor behavioral systems unique framework	Proposed algorithm handles DG related intrinsic issues	IEEE 13-bus/normal config.	Identifies topology changes using D-PMU data	Proper tuning of threshold level is needed for accuracy	Intrusion attack
	61	SBR quantification	RC-SBR	Application of attack against micro-PMUs	DG penetration not considered	IEEE 33-bus/normal config.	Direction of incorrect PMU location finding	Requirement of historical data	Micro-PMU attack
	62	SBR quantification	EC-SBR	No requirement of the number and location of impacted micro-PMUs	Impact of DG not considered	Phasor model of New England-New York system	Network changes obtained by topology processor	Uncorrelated PMU signals may cause error	PMU data corruption attack
	29	SBR miscellaneous	EC-SBR	Processed synchrophasors for anomaly detection	Resilience metric captures impact on DG and critical load	Industrial feeders	Network topology information improves smart grid resilience	Feasible for radial networks	D-PMU data corruption
	87	SBR model based	EC-SBR	Monitoring and accessing PMU bad data detection	DG based largest observable island estimation	Data of peak Reliability synchrophasor project	Observability results changes on topology change	Implementation of ROSE application for SBR improvement	PMU bad data injection
	43	SBR model based	EC-SBR	Rapid identification of data unavailability	DG assists in developing interference strategies	WSCC 9-bus model/normal config.	Post-mortem analysis using topology	Maloperation of protective devices not considered	DoS attack

(Continues)

TABLE 8 (Continued)

Issues		Network parameters										HILF event stage
Ref	Method used	SBR type	Methodology features	Impact on DG	System/Config-ration	Topology identification	Limitations	Based on attack type				
45	SBR model based	EC-SBR	Reconstruction of the data at the corrupted positions itself	Impact on DG not considered	Phasor model of New England-New York system	Topology information considered to select appropriate subspace	Communication layer security un-addressed	Malicious data corruption				After HILF event
47	SBR model based	RC-SBR	Reduced synchrophasor data for SA	DG and communication system aids in mitigation	Guangdong power system case	Cyber event location using network topology	Average performance in terms of time of resilience calculation	PMU data corruption				Before HILF event
48	SBR model based	RC-SBR	Accurate data corruption and reconstruction	DG impacts critical inter-area disruption mitigation	Phasor model of 5-area test system	Temporal proximity results in non-linearity due to injection attack	Large deviation in estimates obtained from corrupted signal	PMU data corruption				After HILF event
51	SBR data driven	EC-SBR	Prediction of failures based on dynamic state monitoring	Intermittent DG sources lead to grid operation close to its security margins	Dataset of American power system	Improves measurement errors due to topology change	With re-initialization of data, efficiency reduces	False data injection				During HILF event
52	SBR data driven	RC-SBR	Stochastic subspace selection for synchrophasor anomaly correction	DG impacts recovery of post-event transients	Phasor model of 5 – area test system	Topology changes addressed by stochastic subspace	Not suitable for coordinated attacks	PMU data corruption				After HILF event
54	SBR machine learning	EC-SBR	Slow changing spatial-temporal pattern under FDI	Impact of DG not considered	IEEE 13, 123-bus/normal config.	Topology information used to develop cyber-attack templates	Cyber-attacks with complex spatial and temporal relationship can be challenging	False data injection				During HILF event
56	SBR machine learning	EC-SBR	Cyber-physical system FDI attack classification from offline small dataset	DG ensures stable operation during mitigation	Data set of Jilin City, China project	Focuses on interaction between electric flow and communication information	With larger system the data variables tend to increase	False data injection				Before HILF event

TABLE 8 (Continued)

Network parameters										
Issues	Ref	Method used	SBR type	Methodology features	Impact on DG	System/Configu-ration	Topology identification	Limitations	Based on attack type	HILF event stage
	64	SBR miscellaneous	RC-SBR	Errors of data to predict restorative actions accurately	Impact of DG not considered	PMU measurements from WECC	Topology information used for locating PMU redundancy	Redundant measurement cases	PMU data injection	During and after HILF event
Combined infrastructure, operational and other anomaly	46	SBR model based	EC-SBR	Distinct key feature of sub-station attack	DG integration offers only short-term operational solution	Ukraine attack case study	Topology emulation for obtaining dynamic properties	Hard to automate all response process	Substation attack	Before HILF event
	50	SBR data driven	EC-SBR	Topology based real-time state estimation	Hybrid SE accurately captures system changes under DERs	IEEE 33-bus/optimal config.	SE model trained under different system topologies	Execution time can be enhanced	PMU data injection	During HILF event
	55	SBR machine learning	RC-SBR	Feature extraction and classification of natural and cyber-related events	Impact of DG not considered	Real dataset of 37 sub-types of attack	Dataset formation based on topology information	Temporal information can improve feature extraction	Intrusion attack	Before HILF event
	57	SBR quantification	RC-SBR	Cost and recovery control decision for cyber-physical system	DG assists in contingency management	Real-time data set from Electric Reliability test system	Cyber asset exploitability values calculated from topology	Attacker patterns cannot be analyzed	Cyber-physical infrastructure attack	After HILF event
	59	SBR quantification	EC-SBR	Unlabeled data to quantify control of uncertainties	DG increases power flow limit to reduce the system risk	RTS-79 test system/optimal config.	Optimal topology reduces cyber-physical cascading failure	System dynamic performance not included	Weather/Cyber-physical system failure	During HILF event
	60	SBR miscellaneous	EC-SBR	Quantification of less popular events such as fires, geo-magnetic issues	DG improves load restoration	System config. Not considered	Topology identification not addressed	Economic perspective can be a challenge in planning	Cyber-physical attack	Before, during and after HILF event

(Continues)

TABLE 8 (Continued)

Network parameters										
Issues	Ref	Method used	SBR type	Methodology features	Impact on DG	System/Configu-ration	Topology identification	Limitations	Based on attack type	HILF event stage
	63	SBR miscellaneous	EC-SBR	Cyber security of PMU and its communication links	Power angle of DGs used to calculate stability during FDIA	IEEE 34-bus/optimal config.	Topology aids in data flow decision	Requirement of control protocols	False data injection	During HILF event
	88	SBR data driven	EC-SBR	Resiliency based preevent system reconfiguration with islanding as a proactive mechanism	DG improves grid resilience	Industrial feeders	DG with topology information improves resilience	Distribution system is at the risk of being unintentionally islanded	False data injection	Before HILF event
	89	SBR machine learning	RC-SBR	Design of complex attack detection criteria using ML techniques	Impact of DG not considered	Data set of IEEE 9-bus test system	Historical data with topology details considered in evaluation	Massive historical records needed for pattern recognition	Data anomaly	During HILF event

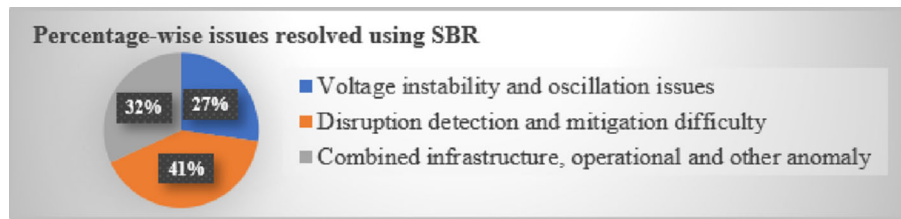


FIGURE 20 Percentage-wise details of issues solved using SBR

TABLE 9 Comparative assessment of SBR methods based on its features

SBR Methods	Data Accuracy	Sample Efficiency	Simulation Results	Merits	Demerits
SBR model based	Depends on operational data and tuning of system data to ensure accuracy, <sup>43,44,90</sup>	Moderate due to dynamic characteristics of system and heavy burden of synchrophasors <sup>47</sup>	The error in the reconstructed synchrophasor data is higher at the beginning of the window, but is acceptable for most of the time span <sup>43-48</sup>	Aptly shows system interdependency due to HILF without making changes in existing infrastructure <sup>48</sup>	At times good pretraining data for implementing in proactive resilience strategy <sup>43-46</sup>
SBR data driven	Accurately captures the maximum deviation level for coarse system changes due to HILF <sup>50,51,53</sup>	The sample efficiency is high but at times are vulnerable to bad data <sup>53</sup>	Data corruption-resilience tested successfully for anomaly ranging from 20% to 50%. <sup>49-53</sup>	Tracks fast system variations of operational states against malicious data <sup>52</sup>	Requires availability and the use of synchrophasor data from larger numbers of PMUs <sup>50,51</sup>
SBR machine learning	Results have dependency on synchrophasor sample data quality <sup>54</sup>	60 extracted features is recommended for the best sample efficiency of 90.48% <sup>59</sup>	The simulation results shows efficiency in terms of total accuracy (95.46%), average precision (95.23%), and average recall (95.97%) values <sup>54-56</sup>	Focuses on input-output relationship of system to reflect network condition <sup>54,56</sup>	Might require good training data to reduce calculation time and decision-making <sup>55</sup>
SBR quantification	Accurate resilience results with a clear interpretation of network characteristics <sup>57-59</sup>	Throughout value, $q = 0.1$ estimates correct classification of the corrupted data for an efficient sampling <sup>58,62</sup>	Results show successful reconstruction of original data from 20% of total number corrupted signals at any instant. <sup>57-61</sup>	Mostly does not require any physical model description for evaluating resilience <sup>60-62</sup>	At times high computation complexity if many integer variables are involved <sup>10,60</sup>
SBR miscellaneous	Accuracy mostly depends on system observability <sup>29</sup>	Data augmentation may increase efficiency <sup>64</sup>	The results show dependency on control and communication system for resilience <sup>29,63,64,91</sup>	Resilience can be captured from different system aspects <sup>29,64</sup>	SBR estimation at different time horizons is mostly not possible <sup>64</sup>

Hence, fault diagnoses can be performed efficiently using synchrophasor data in prevent condition and using UAV for difficult to reach areas. It will enhance overall system resilience.<sup>99</sup> Figure 21 represents the distribution line status monitoring method.

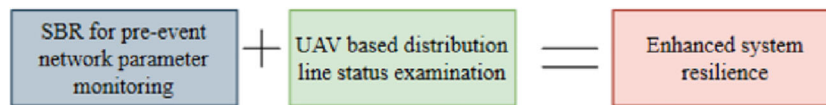


FIGURE 21 Enhancement of weather-dependent SBR for an evolving distribution system

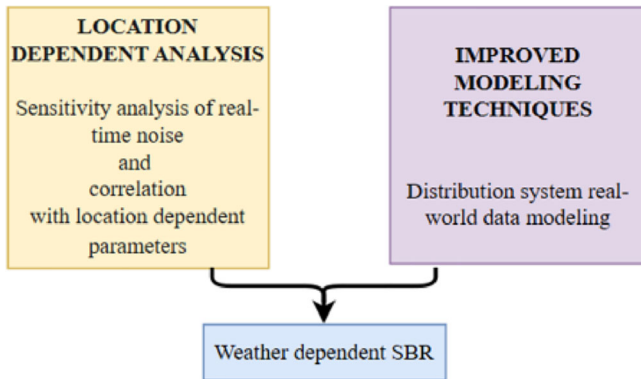


FIGURE 22 Resilience enhancement model using combinatorial analysis

- ii. The synchrophasor measurements experience inconsistency during data injection and other related cyber-attacks.<sup>100,101</sup> Sometimes negligible data injection impacts system operation. A method will be imperative to analyze these minute levels of imbalances in distribution systems to increase the accuracy.
- iii. The existing methods of weather-dependent SBR are mainly based on fast detection strategies, identification of grid disturbances, its classification, and its corrective actions.<sup>102-105</sup> A sensitivity analysis of real-time noise, correlation with location dependent parameters and their impact on the performance of different modeling techniques is necessary before deciding the most suitable enhancement strategy. Figure 22 represents the modeling of synchrophasor data for an improved resilience analysis.

- iv. Proactive resilience analysis consists of three main steps, which are continuous online monitoring, prediction of failures, and timely mitigation.<sup>106-109</sup> There is a requirement of multi-HILF event resilience enhancement strategy so that resilience measures for a particular event may not interfere with the approach of another such adverse event.

The above discussed future aspects can be availed to study and analyze the SBR of the distribution system with a focus on a holistic, temporal, and variable HILF risk assessment framework for choosing the best strategy to be executed.

## 9 | CONCLUSION

SBR is incorporated for a fairly improved real-time visualization, monitoring, control, and analysis of system parameters against HILF events. These attributes contribute to better understanding of the system's vulnerabilities and enhances SA, which makes it less likely to succumb to the adverse events. SBR improvement methods offer a novel solution enabling quick diagnosis as well as timely restoration by adding value to the decision-making process and also an insightful post-event forensic study. This review represents an attempt to seek an overview of synchrophasor technology-oriented distribution system resilience. It provides insight into the resilience framework concept using micro-PMU, discusses the issues encountered by the distribution system in response to which synchrophasor based resilience concept is beneficial, and synchrophasor based methods for distribution system resilience enhancement. From the analysis, it may be deduced that the SBR model based as well as the SBR quantification approach seems to be the two dominant areas where most of the synchrophasor based resilience techniques are applied. To impose SBR, different methods are considered in literature such as the SBR model approach, SBR data-driven approach, SBR machine learning approach, SBR quantification methods, and SBR miscellaneous approach. Appropriate mathematical

formulations are provided to support the different suggested methods. A detailed comparison covering issues due to HILF events in the distribution system, methods used to implement SBR, along with attributes of SBR methods are specified. The review further suggests possible prospects that can be used to realize distribution system resilience using synchrophasor technology along with unmanned aerial systems and improved real-world modeling techniques for more accurate and detailed analysis under incident based extreme weather scenarios, cyber-attacks, and many such complex cyber-physical conditions.

## PEER REVIEW

The peer review history for this article is available at <https://publons.com/publon/10.1002/2050-7038.12934>.

## DATA AVAILABILITY STATEMENT

Data sharing not applicable - no new data generated

## ORCID

Sonal  <https://orcid.org/0000-0001-8238-4308>

Debomita Ghosh  <https://orcid.org/0000-0001-8942-8828>

## REFERENCES

1. Mohamed MA, Chen T, Su W, Jin T. Proactive resilience of power systems against natural disasters: a literature review. *IEEE Access*. 2019;7:163778-163795.
2. Alizadeh MI, Parsa Moghaddam M, Amjady N, Siano P, Sheikh-El-Eslami MK. Flexibility in future power systems with high renewable penetration: a review. *Renewable Sustain Energy Rev*. 2016;57:1186-1193.
3. Wang Y, Chen C, Wang J, Baldick R. Research on resilience of power systems under natural disasters—a review. *IEEE Trans Power Syst*. 2016;31(2):1604-1613.
4. Clark A, Zonouz S. Cyber-physical resilience: definition and assessment metric. *IEEE Trans Smart Grid*. 2019;10(2):1671-1684.
5. Australian Bureau of Statistics. Consumer Price Index, Australia, June 2018, cat. no. 6401.1, Canberra, 2018.
6. Raoufi H, Vahidinasab V, Mehran K. Power systems resilience metrics: a comprehensive review of challenges and outlook. *Sustainability*. 2020;12(22):9698.
7. Bessani M, Massignan JAD, Fanucchi RZ, et al. Probabilistic assessment of power distribution systems resilience under extreme weather. *IEEE Syst J*. 2019;13(2):1747-1756.
8. Poudel S, Dubey A, Bose A. Risk-based probabilistic quantification of power distribution system operational resilience. *IEEE Syst J*. 2020;14(3):3506-3517.
9. Sabouhi H, Doroudi A, Fotuhi-Firuzabad M, Bashiri M. Electrical power system resilience assessment: a comprehensive approach. *IEEE Syst J*. 2020;14(2):2643-2652.
10. Wang Q, Yu Z, Ye R, Lin Z, Tang Y. An ordered curtailment strategy for offshore wind power under extreme weather conditions considering the resilience of the grid. *IEEE Access*. 2019;7:54824-54833.
11. Dehghani NL, Mohammadi Darestani Y, Shafieezadeh A. Optimal life-cycle resilience enhancement of aging power distribution systems: a MINLP-based preventive maintenance planning. *IEEE Access*. 2020;8:22324-22334.
12. Panteli M, Mancarella P. The grid: stronger, bigger, smarter?: presenting a conceptual framework of power system resilience. *IEEE Power Energy Mag*. 2015;13(3):58-66.
13. Nazemi M, Moeini-Aghtaie M, Fotuhi-Firuzabad M, Dehghanian P. Energy storage planning for enhanced resilience of power distribution networks against earthquakes. *IEEE Trans Sustain Energy*. 2020;11(2):795-806.
14. Salimi M, Nasr M-A, Hosseinian SH, Gharehpetian GB, Shahidehpour M. Information gap decision theory-based active distribution system planning for resilience enhancement. *IEEE Trans Smart Grid*. 2020;11(5):4390-4402.
15. Tabatabaei NM, Ravadanegh SN, Bizon N. *Power Systems Resilience: Modeling Analysis and Practice*. Cham, Switzerland: Springer; 2019.
16. Office of Electricity Delivery and Energy Reliability, U.S. Department of Energy. “Electric Disturbance Events (OE-417). Accessed September 2015. <http://www.oe.netl.doe.gov/oe417.aspx>.
17. Electric power transmission and distribution losses, EA Statistics, OECD/IEA, 2018, <https://data.worldbank.org/indicator/EG.ELC.LOSS.ZS>.
18. Kahan H, Allen AC, George JK. An operational framework for resilience. *J Homeland Secur Emerg Manag*. 2009;6(1):1547-7355.
19. Berkeley AR, Wallace M, Coe C. A framework for establishing critical infrastructure resilience goals. Nat Infrastruct Advisory Council, Washington, DC, USA, 2010. [Online]. <http://www.dhs.gov/xlibrary/assets/niac/niac-a-framework-for-establishing-critical-infrastructure-resilience-goals-2010-10-19.pdf>.
20. Woods DD. Four concepts for resilience and the implications for the future of resilience engineering. *Rel Eng Syst Saf*. 2015;141:5-9.
21. Chanda S, Srivastava AK. Defining and enabling resiliency of electric distribution systems with multiple microgrids. *IEEE Trans Smart Grid*. 2016;7(6):2859-2868.

22. Mc Daniels T, Chang S, Cole D, Mikawoz J, Longstaff H. Fostering resilience to extreme events within infrastructure systems: characterizing decision contexts for mitigation and adaptation. *Glob Environ Chang*. 2008;18(2):310-318.
23. Mahzarnia M, Moghaddam MP, Baboli PT, Siano P. A review of the measures to enhance power systems resilience. *IEEE Syst J*. 2020;14(3):4059-4070.
24. Schneider KP, Tuffner FK, Elizondo MA, Liu C, Xu Y, Ton D. Evaluating the feasibility to use microgrids as a resiliency resource. *IEEE Trans Smart Grid*. 2017;8(2):687-696.
25. Rodríguez H, Aguirre B. Hurricane Katrina and the healthcare infrastructure: a focus on disaster preparedness, response, and resiliency. *Front Health Serv Manag*. 2006;231:13-23.
26. Ma S, Su L, Wang Z, Qiu F, Guo G. Resilience enhancement of distribution grids against extreme weather events. *IEEE Trans Power Syst*. 2018;33(5):4842-4853.
27. Fanucchi RZ et al. Stochastic indexes for power distribution systems resilience analysis. *IET Generation, Transmission & Distribution*. 2019;13(12):2507-2516.
28. Xu Y, Liu C, Schneider KP, Tuffner FK, Ton DT. Microgrids for service restoration to critical load in a resilient distribution system. *IEEE Trans Smart Grid*. 2018;9(1):426-437.
29. Pandey S, Chanda S, Srivastava AK, Hovsopian RO. Resiliency-driven proactive distribution system reconfiguration with Synchrophasor data. *IEEE Trans Power Syst*. 2020;35(4):2748-2758.
30. 2021 Cyber Security Statistics The Ultimate List Of Stats, 2021. <https://purplesec.us/resources/cyber-security-statistics/>.
31. World Bank Enterprise Surveys Data. February 22, 2017, <https://www.enterprisesurveys.org/Data>.
32. Gao H, Chen Y, Mei S, Huang S, Xu Y. Resilience-oriented pre-hurricane resource allocation in distribution systems considering electric buses. *Proc IEEE*. 2017;105(7):1214-1233.
33. Arghandeh R, von Meier A, Mehrmanesh L, Mili L. On the definition of cyber-physical resilience in power systems. *Renewable Sustain Energy Rev*. 2016;58:1060-1069.
34. Han SR. *Estimating Hurricane Outage and Damage Risk in Power Distribution Systems*. College Station, TX: Texas A&M Univ; 2008.
35. Van de Vyver J, Deconinck G, Belmans R. The need for a distributed algorithm for control of the electrical power infrastructure. In: *The 3rd International Workshop on Scientific Use of Submarine Cables and Related Technologies*, Lugano, Switzerland, 2003, 211-215.
36. Bie Z, Lin Y, Li G, Li F. Battling the extreme: a study on the power system resilience. *Proc IEEE*. 2017;105(7):1253-1266.
37. O'Rourke TD. Critical infrastructure, interdependencies, and resilience. *Bridg Acad Eng*. 2007;37(1):22-29.
38. Panteli M, Pickering C, Wilkinson S, Dawson R, Mancarella P. Power system resilience to extreme weather: fragility modeling, probabilistic impact assessment, and adaptation measures. *IEEE Trans Power Syst*. 2017;32(5):3747-3757.
39. Nguyen T, Wang S, Alhazmi M, Nazemi M, Estebarsari A, Dehghanian P. Electric power grid resilience to cyber adversaries: state of the art. *IEEE Access*. 2020;8:87592-87608.
40. Yuan W, Wang J, Qiu F, Chen C, Kang C, Zeng B. Robust optimization-based resilient distribution network planning against natural disasters. *IEEE Trans Smart Grid*. 2016;7(6):2817-2826.
41. Buque C, Chowdhury S. Distributed generation and microgrids for improving electrical grid resilience: review of the Mozambican scenario. *Proc Power Energy Soc General Meet*. 2016;2016(1):1-5.
42. Zarakas WP, Sergici S, Bishop H, Zahniser-Word J, Fox-Penner P. Utility investments in resiliency: balancing benefits with cost in an uncertain environment. *Electrical J*. 2014;27(5):31-41.
43. Chawla A, Agrawal P, Singh A, Panigrahi BK, Paul K, Bhalja B. Denial-of-service resilient frameworks for Synchrophasor-based wide area monitoring systems. *Computer*. 2020;53(5):14-24.
44. Zhang Y, Wang J, Liu J. Attack identification and correction for PMU GPS spoofing in unbalanced distribution systems. *IEEE Trans Smart Grid*. 2020;11(1):762-773.
45. Mahapatra K, Ashour M, Chaudhuri NR, Lagoa CM. Malicious corruption resilience in PMU data and wide-area damping control. *IEEE Trans Smart Grid*. 2020;11(2):958-967.
46. Tan HC, Cheh C, Chen B, Mashima D. Tabulating cybersecurity solutions for substations: towards pragmatic design and planning. In: *2019 IEEE Innovative Smart Grid Technologies - Asia (ISGT Asia)*, Chengdu, China, 2019, 1018-1023.
47. Liu S et al. Data-driven event detection of power systems based on unequal-interval reduction of PMU data and local outlier factor. *IEEE Trans Smart Grid*. 2020;11(2):1630-1643.
48. Mahapatra K, Chaudhuri NR. Malicious corruption-resilient wide-area oscillation monitoring using principal component pursuit. *IEEE Trans Smart Grid*. 2019;10(2):1813-1825.
49. Farajollahi M, Shahsavari A, Stewart E, Mohsenian-Rad H. Locating the source of events in power distribution systems using micro-PMU data. *2019 IEEE Power & Energy Society General Meeting (PESGM)*, Atlanta, GA, USA, 2019, 1-1.
50. Huang M, Wei Z, Sun G, Zang H. Hybrid state estimation for distribution systems with AMI and SCADA measurements. *IEEE Access*. 2019;7:120350-120359.
51. Chakhchoukh Y, Lei H, Johnson BK. Diagnosis of outliers and cyber attacks in dynamic PMU-based power state estimation. *IEEE Trans Power Syst*. 2020;35(2):1188-1197.
52. Chatterjee K, Mahapatra K, Chaudhuri NR. Robust recovery of PMU signals with outlier characterization and stochastic subspace selection. *IEEE Trans Smart Grid*. 2020;11(4):3346-3358.
53. Mayo-Maldonado JC et al. Data-driven framework to model identification, event detection, and topology change location using D-PMUs. *IEEE Trans Instrumen Measur*. 2020;69(9):6921-6933.

54. Cui M, Wang J, Chen B. Flexible machine learning-based cyberattack detection using spatiotemporal patterns for distribution systems. *IEEE Trans Smart Grid*. 2020;11(2):1805-1808.
55. Hu C, Yan J, Wang C. Robust feature extraction and ensemble classification against cyber-physical attacks in the smart grid. 2019 IEEE Electrical Power and Energy Conference (EPEC), Montreal, QC, Canada, 2019, 1-6.
56. Cao J et al. A novel false data injection attack detection model of the cyber-physical power system. *IEEE Access*. 2020;8:95109-95125.
57. Venkataramanan V, Hahn A, Srivastava A. CyPhyR: a cyber-physical analysis tool for measuring and enabling resiliency in microgrids. *IET Cyber-Phys Syst Theory Appl*. 2019;4(4):313-321.
58. Cui Q, Weng Y. Enhance high impedance fault detection and location accuracy via - PMUs. *IEEE Trans Smart Grid*. 2020;11(1):797-809.
59. Liu Y, Lu D, Deng L, Bai T, Hou K, Zeng Y. Risk assessment for the cascading failure of electric cyber-physical system considering multiple information factors. *IET Cyber-Physical Syst Theory Appl*. 2017;2(4):155-160.
60. Haggi H, Nejad RR, Song M, Sun W. A review of smart grid restoration to enhance cyber-physical system resilience. In 2019 IEEE Innovative Smart Grid Technologies - Asia (ISGT Asia), Chengdu, China, 2019, 4008-4013.
61. Kamal M, Farajollahi M, Mohsenian-Rad H. Analysis of cyber attacks against micro-PMUs: the case of event source location identification. In: 2020 IEEE Power & Energy Society Innovative Smart Grid Technologies Conference (ISGT), Washington DC, USA, 2020, 1-5.
62. Mahapatra K, Chaudhuri NR. Online robust PCA for malicious attack-resilience in wide-area mode metering application. *IEEE Trans Power Syst*. 2019;34(4):2598-2610.
63. Bidram B, Poudel L, Damodaran RF, Guerrero JM. Resilient and Cybersecure distributed control of inverter-based islanded microgrids. *IEEE Trans Ind Inform*. 2020;16(6):3881-3894.
64. Wang S, Zhao J, Huang Z, Diao R. Assessing Gaussian assumption of PMU measurement error using field data. *IEEE Trans Power Deliv*. 2018;33(6):3233-3236.
65. Khalid HM, Peng JC. A Bayesian algorithm to enhance the resilience of WAMS applications against cyber attacks. *IEEE Trans Smart Grid*. 2016;7(4):2026-2037.
66. Musleh AS, Khalid HM, Muyeen SM, Al-Durra A. A prediction algorithm to enhance grid resilience toward cyber attacks in WAMCS applications. *IEEE Syst J*. 2019;13(1):710-719.
67. Wang X, Yaz EE. Smart power grid synchronization with fault tolerant nonlinear estimation. *IEEE Trans Power Syst*. 2016;31(6):4806-4816.
68. Chen C, Wang J, Ton D. Modernizing distribution system restoration to achieve grid resiliency against extreme weather events: an integrated solution. *Proc IEEE*. 2017;105(7):1267-1288.
69. Wang Y et al. Coordinating multiple sources for service restoration to enhance resilience of distribution systems. *IEEE Trans Smart Grid*. 2019;10(5):5781-5793.
70. Li Z, Shahidehpour M, Aminifar F, Alabdulwahab A, Al-Turki Y. Networked microgrids for enhancing the power system resilience. *Proc IEEE*. 2017;105(7):1289-1310.
71. Liu W, Lin Z, Wen F, Ledwich G. A wide area monitoring system based load restoration method. *IEEE Trans Power Syst*. 2013;28(2):2025-2034.
72. Guo Y, Li K, Laverty DM, Xue Y. Synchrophasor-based islanding detection for distributed generation systems using systematic principal component analysis approaches. *IEEE Trans Power Deliv*. 2015;30(6):2544-2552.
73. Zhou M, Wang Y, Srivastava AK, Wu Y, Banerjee P. Ensemble-based algorithm for Synchrophasor data anomaly detection. *IEEE Trans Smart Grid*. 2019;10(3):2979-2988.
74. Xu Y et al. DGs for service restoration to critical loads in a secondary network. *IEEE Trans Smart Grid*. 2019;10(1):435-447.
75. Golshani A, Sun W, Zhou Q, Zheng QP, Hou Y. Incorporating wind Energy in power system restoration planning. *IEEE Trans Smart Grid*. 2019;10(1):16-28.
76. Aktarujjaman M, Kashem MA, Negnevitsky M, Ledwich G. "Black Start with Dfig Based Distributed Generation after Major Emergencies," 2006 International Conference on Power Electronic. New Delhi: Drives and Energy Systems; 2006.
77. Zhu H, Liu Y. Aspects of power system restoration considering wind farms. In: international conference on sustainable power generation and supply (SUPERGEN 2012), Hangzhou, 2012, 2012, 1-5.
78. Nezam Sarmadi SA, Dobakhshari AS, Azizi S, Ranjbar AM. A sectionalizing method in power system restoration based on WAMS. *IEEE Trans Smart Grid*. 2011;2(1):190-197.
79. Shahsavari A, Farajollahi M, Stewart EM, Cortez E, Mohsenian-Rad H. Situational awareness in distribution grid using micro-PMU data: a machine learning approach. *IEEE Trans Smart Grid*. 2019;10(6):6167-6177.
80. Bajpai P, Chanda S, Srivastava AK. A novel metric to quantify and enable resilient distribution system using graph theory and Choquet integral. *IEEE Trans Smart Grid*. 2018;9(4):2918-2929.
81. Huang G, Wang J, Chen C, Qi J, Guo C. Integration of preventive and emergency responses for power grid resilience enhancement. *IEEE Trans Power Syst*. 2017;32(6):4451-4463.
82. Zertek A, Verbic G, Pantos M. A novel strategy for variable-speed wind Turbines' participation in primary frequency control. *IEEE Trans Sustainable Energy*. 2012;3(4):791-799.
83. Gou B, Kavasseri RG. Unified PMU placement for observability and bad data detection in state estimation. *IEEE Trans Power Syst*. 2014;29(6):2573-2580.
84. Tushar S, Pandey A, Srivastava K, Markham P, Patel M. Online estimation of steady-state load models considering data anomalies. *IEEE Trans Industry Appl*. 2018;54(1):712-721.

85. Gholami A, Aminifar F. A hierarchical response-based approach to the load restoration problem. *IEEE Trans Smart Grid*. 2017;8(4):1700-1709.
86. Hou Y, Liu C, Sun K, Zhang P, Liu S, Mizumura D. Computation of milestones for decision support during system restoration. *IEEE Trans Power Syst*. 2011;26(3):1399-1409.
87. Vaiman M, Energy V, Vaiman M. Use of PMU-based framework to improve power system resilience and reliability. In: 2018 IEEE International Conference on Probabilistic Methods Applied to Power Systems (PMAPS), Boise, ID, 2018: 1-6.
88. Liang G, Weller SR, Zhao J, Luo F, Dong ZY. The 2015 Ukraine blackout: implications for false data injection attacks. *IEEE Trans Power Syst*. 2017;32(4):3317-3318.
89. Wang J, Shi D, Li Y, Chen J, Ding H, Duan X. Distributed framework for detecting PMU data manipulation attacks with deep autoencoders. *IEEE Trans Smart Grid*. 2019;10(4):4401-4410.
90. Rodrigues YR, Abdelaziz MMA, Wang L. Resilience-oriented D-PMU based frequency controller for islanded microgrids with flexible resources support. *IEEE Trans Power Deliv*. 2020;99:1-1. <https://doi.org/10.1109/TPWRD.2020.3047653>.
91. Proceedings of 1st International Conference on Landslides Risk reduction and Resilience 2019, New Delhi, India, 28th November, 2019. [https://nidm.gov.in/PDF/pubs/28thLRR\\_Report.pdf](https://nidm.gov.in/PDF/pubs/28thLRR_Report.pdf).
92. von Meier A, Arghandeh R. Every moment counts: synchrophasors for distribution networks with variable resources. *Renewable Energy Integration*. 2nd ed. Cambridge, MA: Elsevier; 2017:435-444.
93. Kandaperumal G, Srivastava AK. Resilience of the electric distribution systems: concepts, classification, assessment, challenges, and research needs. *IET Smart Grid*. 2020;3(2):133-143.
94. Sundararajan A, Khan T, Moghadasi A, Sarwat AI. Survey on synchrophasor data quality and cybersecurity challenges, and evaluation of their interdependencies. *J Modern Power Syst Clean Energy*. 2019;7(3):449-467.
95. Gholami A, Shekari T, Amiroun MH, Aminifar F, Amini MH, Sargolzaei A. Toward a consensus on the definition and taxonomy of power system resilience. *IEEE Access*. 2018;6:32035-32053.
96. U.S. Department of Energy. Recovery Act: Smart Grid Investment Grant (SGIG) Program, 2016. [Online]. <http://energy.gov/oe/information-center/recoveryact-smart-grid-investment-grant-sgigprogram>.
97. GTM Research. The new face of damage assessment, 2015. [Online]. <http://www.ourenergypolicy.org/wp-content/uploads/2016/01/GE-Whitepaper-2015-Web-Final.pdf>.
98. Alam MM, Zhu Z, Eren Tokgoz B, et al. Automatic assessment and prediction of the resilience of utility poles using unmanned aerial vehicles and computer vision techniques. *Int J Disaster Risk Sci*. 2020;11:119-132.
99. Liu H, Davidson RA, Rosowsky DV, Stedinger JR. Negative binomial regression of electric power outages in hurricanes. *J Infrastruct Syst*. 2005;11(4):258-267.
100. Eisele S, Mardari I, Dubey A, Karsai G. RIAPS: resilient information architecture platform for decentralized smart systems. In: 2017 IEEE 20th International Symposium on Real-Time Distributed Computing (ISORC), Toronto, ON, 2017, 125-132.
101. Jamei M et al. Micro Synchrophasor-based intrusion detection in automated distribution systems: toward critical infrastructure security. *IEEE Internet Comput*. 2016;20(5):18-27.
102. IEEE Guide for Design, Operation, and Integration of Distributed Resources Island Systems With Electric Power Systems, Coordinating Committee 21 on Fuel Cells, Photovoltaics, Dispersed Generation, and Energy Storage, *IEEE Standards 1547.42011*, 2011.
103. Sun K, Chen Q, Gao Z. An automatic faulted line section location method for electric power distribution systems based on multisource information. *IEEE Trans Power Deliv*. 2016;31(4):1542-1551.
104. Wang J. Advanced distribution management systems for grid modernization: DMS functions. Argonne Nat. Lab., Lemont, IL, USA, Tech. Rep. ANL/ESD-15/17, 2015.
105. Küfeoglu S. *Economic impacts of electric power outages and evaluation of customer interruption costs*. [Ph.D. dissertation] Aalto Univ., Espoo, Finland; 2015.
106. Zhou D et al. Distributed data analytics platform for wide-area synchrophasor measurement systems. *IEEE Trans Smart Grid*. 2016;7(5):2397-2405.
107. Khan R, Maynard P, McLaughlin K, Laverty D, Sezer S. Threat analysis of black energy malware for synchrophasor based real-time control and monitoring in smart grid. In: 4th International Symposium for ICS & SCADA Cyber, 2016.
108. Seca L, Costa H, Moreira CL, Lopes JAP. An innovative strategy for power system restoration using utility scale wind parks. In: 2013 IREP Symposium Bulk Power System Dynamics and Control - IX Optimization, Security and Control of the Emerging Power Grid, Rethymno, 2013: 1-8.
109. Srivastava A, Pandey S, Zhou M, Banerjee P, Wu Y. Ensemble based technique for synchrophasor data quality and analyzing its impact on applications. In: North American Synchrophasor Initiative (NASPI), Gaithersburg, MD, 2017: 1-24.

**How to cite this article:** Sonal, Ghosh D. Novel trends in resilience assessment of a distribution system using synchrophasor application: A literature review. *Int Trans Electr Energy Syst*. 2021;31:e12934. <https://doi.org/10.1002/2050-7038.12934>